heparin sulfates might not be expressed in the cells in the inside of islets. The fact of distinct CAR expression in mouse β-cell line MIN6 cells (Fig. 1A) also supports this assumption.

Transduction efficiency in fresh islets with the conventional Ad vector was equal to that in overnight-cultured islets (data not shown), suggesting that a low level of CAR expression in fresh islets would be enough for Ad infection. The reason why CAR expression in islets was enhanced by cultivation is unknown. Because it has been reported that CAR expression is enhanced by long term culture or influenced by culture medium in cardiomyocytes [29,30], same mechanism might work in islet cells. Ad vector-mediated gene expression *in vitro* lasts for a long term if the cells do not divide. Since islets do not proliferate *in vitro* and can be cultured for only a few days, gene expression would last throughout the duration of islet culture.

To overcome the physical problem of Ad infection into the cells in the inside of islets, we examined the effect of Ca^{2+}-free condition in which cell-to-cell adhesion becomes weak on Ad vector transduction into islets. Fig. 2A shows that preincubation in Ca^{2+}-free buffer for 15 min before transduction with Ad-CALacZ effectively enhanced β-galactosidase activity of islets. However, confocal microscopic analyses did not reveal distinct enhancement of transduction efficiency especially in the inside of islets (Fig. 2B). The Ca^{2+}-free treatment or collagenase digestion which makes cell-to-cell adhesion weak has a limitation because excessive treatments destroy the form of the islet.

Pancreatic islets are one of the most vascularized organs of the body. The density of the islet capillary network and blood flowing through the islets is about five times greater than that in exocrine pancreatic tissue [31,32]. This probably reflects the requirements of the islets for rich supplies of nutrients and oxygen, as well as for rapid disposal of metabolites and secreted hormones. We next tried Ad vector transduction through blood vessels that branch into the islet capillary network to obtain more efficient gene transduction, especially into the inside of islets. The celiac artery branched from the abdominal aorta is upper and proximal vessel toward the pancreas (Fig. 3A). After ligation of the hepatic artery with the portal vein and the splenic artery, respectively, Ad-CAGFP was injected through the celiac artery (Fig. 3A). Isolated islets were cultured, and their transgene expression was evaluated. As shown in Fig. 3B and

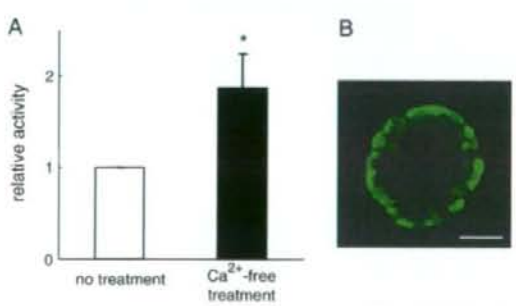

Fig. 2. Effect of Ca^{2+}-free treatment on Ad vector transduction into pancreatic islets. (A) Mouse islets were preincubated in Ca^{2+}-free KRBB for 15 min before they were transduced with Ad-CALacZ for 1 h. The medium containing the Ad vector was exchanged for fresh medium, and β-galactosidase activity of the islets was measured by luminescence assay 24 h later. The β-galactosidase activity was represented for a ratio to that of untreated islets. The data are expressed as the mean ± S.D. ($n=3$). Statistical significance was evaluated by unpaired Student's t test. $^*p<0.05$ vs. no treatment. (B) Mouse islets were preincubated in Ca^{2+}-free KRBB for 15 min before they were transduced with Ad-CAGFP for 1 h. Confocal microscopic analyses were performed 24 h later. A bar represents 50 μm.

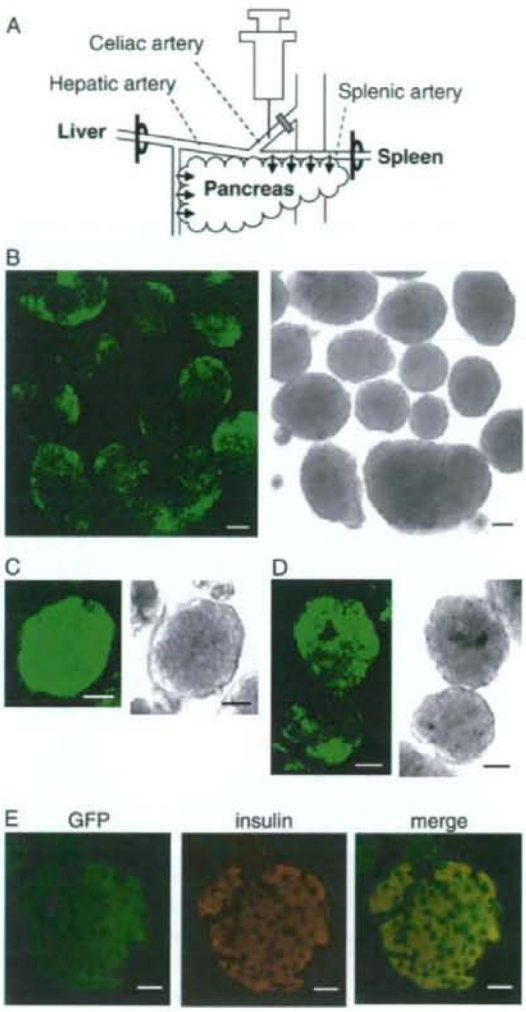

Fig. 3. Ad vector transduction into pancreatic islets *in vivo*. (A) Schema of Ad vector transduction *in vivo*. After ligation of the hepatic artery with the portal vein at the porta hepatis and the splenic artery at the hilum of the spleen, respectively, Ad-CAGFP was injected into the lower side of the clamed point of the celiac artery. Five minutes later, pancreatic islets were isolated and cultured for 24 h. (B–D) Confocal microscopic analyses of pancreatic islets of mice (B, C) and rats (D). An islet expressing GFP throughout the islet (C) was also observed. Each left panel and right panel represents the image of GFP-expressing islets and the corresponding visible image, respectively. Bars represent 50 μm. (E) Immunohistochemical analyses of sliced sections of mouse islets. Paraffin sections of islets were stained using an anti-insulin antibody and visualized with rhodamine. Bars represent 50 μm.

D, Ad vector transduction *in vivo* succeeded in GFP expression in isolated islets. As had been expected, GFP was expressed even in the inside of islets, though not all islets effectively expressed GFP. We also observed that some islets express GFP throughout the islet. A typical image is shown in Fig. 3C. Furthermore, to determine whether β-cells were transduced, immunohistochemical analyses using an anti-insulin antibody were performed (Fig. 3E). Data showed that GFP expression was observed in insulin-producing cells, indicating that β-cells in the inside of islets were indeed transduced.

In vivo gene transfer to pancreatic islets using other routes, such as through the common bile duct [33,34] or a distal blood vessel from the pancreas [35], has been reported. However, the transgene was not expressed in islets efficiently and entirely and its expression pattern within the islet has not been analyzed in detail. This study should be valuable as a description of successful transduction into the inside of islets by the Ad vector.

In the present study, we have shown that pancreatic islets express CAR, a receptor for Ad, but that Ad vector-mediated transgene is expressed only in the periphery of the islets due to physical obstruction. We demonstrated that Ca^{2+}-free treatment before Ad vector transduction improves gene transduction into islets. Furthermore, Ad vector transduction through a proximal blood vessel *in vivo* and then cultivation of islets *in vitro* mediated efficient gene expression even in the inside of islets. Since pancreatic β-cells exist in the inner area of islets, this technique for Ad vector transductions could be very useful for basic research for β-cells and further therapeutic application for diabetes mellitus.

Acknowledgements

We are grateful to Dr. J. Miyazaki for generously providing the CA promoter and MIN6 cells. We also thank Drs. C. Yamada and K. Toyoda for their advice on anatomical techniques. This work was supported by grants for Health and Labour Sciences Research from the Ministry of Health, Labour, and Welfare of Japan.

References

[1] J.L. Gaglia, A.M. Shapiro, G.C. Weir, Islet transplantation: progress and challenge, Arch. Med. Res. 36 (2005) 273–280.
[2] J.R. Lakey, M. Mirbolooki, A.M. Shapiro, Current status of clinical islet cell transplantation, Methods Mol. Biol. 333 (2006) 47–104.
[3] S. Matsumoto, H. Noguchi, Y. Yonekawa, T. Okitsu, Y. Iwanaga, X. Liu, H. Nagata, N. Kobayashi, C. Ricordi, Pancreatic islet transplantation for treating diabetes, Expert Opin. Biol. Ther. 6 (2006) 23–37.
[4] L. Groop, Pathogenesis of type 2 diabetes: the relative contribution of insulin resistance and impaired insulin secretion, Int. J. Clin. Pract. Suppl. (2000) 3–13.
[5] A.J. Scheen, Pathophysiology of type 2 diabetes, Acta Clin. Belg. 58 (2003) 335–341.
[6] H. Basudev, P.M. Jones, S.L. Howell, Protein phosphorylation in the regulation of insulin secretion: the use of site-directed inhibitory peptides in electrically permeabilised islets of Langerhans, Acta Diabetol. 32 (1995) 32–37.
[7] P.Y. Benhamou, C. Moriscot, P. Prevost, E. Rolland, J. Chroboczek, S. Halimi, A methodology for an efficient and reproducible gene transfer into porcine islets using cationic liposomes, Transplant. Proc. 29 (1997) 2203.
[8] J.R. Lakey, A.T. Young, D. Pardue, S. Calvin, T.E. Albertson, L. Jacobson, T.J. Cavanagh, Nonviral transfection of intact pancreatic islets, Cell Transplant 10 (2001) 697–708.
[9] R.I. Mahato, J. Henry, A.S. Narang, O. Sabek, D. Fraga, M. Kotb, A.O. Gaber, Cationic lipid and polymer-based gene delivery to human pancreatic islets, Mol. Ther. 7 (2003) 89–100.
[10] C. Volpers, S. Kochanek, Adenoviral vectors for gene transfer and therapy, J. Gene Med. 6 (Suppl 1) (2004) S164–S171.
[11] H. Mizuguchi, T. Hayakawa, Targeted adenovirus vectors, Hum. Gene Ther. 15 (2004) 1034–1044.
[12] T.C. Becker, H. BeltrandelRio, R.J. Noel, J.H. Johnson, C.B. Newgard, Overexpression of hexokinase I in isolated islets of Langerhans via recombinant adenovirus. Enhancement of glucose metabolism and insulin secretion at basal but not stimulatory glucose levels, J. Biol. Chem. 269 (1994) 21234–21238.
[13] G. Leibowitz, G.M. Beattie, T. Kafri, V. Cirulli, A.D. Lopez, A. Hayek, F. Levine, Gene transfer to human pancreatic endocrine cells using viral vectors, Diabetes 48 (1999) 745–753.
[14] G. Bilbao, J.L. Contreras, I. Dmitriev, C.A. Smyth, S. Jenkins, D. Eckhoff, F. Thomas, J. Thomas, D.T. Curiel, Genetically modified adenovirus vector containing an RGD peptide in the HI loop of the fiber knob improves gene transfer to nonhuman primate isolated pancreatic islets, Am. J. Transplant. 2 (2002) 237–243.
[15] M. Narushima, T. Okitsu, A. Miki, C. Yong, K. Kobayashi, Y. Yonekawa, K. Tanaka, H. Ikeda, S. Matsumoto, N. Tanaka, N. Kobayashi, Adenovirus mediated gene transduction of primarily isolated mouse islets, ASAIO J. 50 (2004) 586–590.
[16] A.R. Barbu, G. Akusjarvi, N. Welsh, Adenoviral-mediated transduction of human pancreatic islets: importance of adenoviral genome for cell viability and association with a deficient antiviral response, Endocrinology 146 (2005) 2406–2414.
[17] H. Mizuguchi, M.A. Kay, Efficient construction of a recombinant adenovirus vector by an improved in vitro ligation method, Hum. Gene Ther. 9 (1998) 2577–2583.
[18] H. Mizuguchi, M.A. Kay, A simple method for constructing E1- and E1/E4-deleted recombinant adenoviral vectors, Hum. Gene Ther. 10 (1999) 2013–2017.
[19] H. Niwa, K. Yamamura, J. Miyazaki, Efficient selection for high-expression transfectants with a novel eukaryotic vector, Gene 108 (1991) 193–199.
[20] J.V. Maizel Jr., D.O. White, M.D. Scharff, The polypeptides of adenovirus. I. Evidence for multiple protein components in the virion and a comparison of types 2, 7A, and 12, Virology 36 (1968) 115–125.
[21] R. Sutton, M. Peters, P. McShane, D.W. Gray, P.J. Morris, Isolation of rat pancreatic islets by ductal injection of collagenase, Transplantation 42 (1986) 689–691.
[22] J.M. Bergelson, J.A. Cunningham, G. Droguett, E.A. Kurt-Jones, A. Krithivas, J.S. Hong, M.S. Horwitz, R.L. Crowell, R.W. Finberg, Isolation of a common receptor for Coxsackie B viruses and adenoviruses 2 and 5, Science 275 (1997) 1320–1323.
[23] T.J. Wickham, E. Tzeng, L.L. Shears II, P.W. Roelvink, Y. Li, G.M. Lee, D.E. Brough, A. Lizonova, I. Kovesdi, Increased in vitro and in vivo gene transfer by adenovirus vectors containing chimeric fiber proteins, J. Virol. 71 (1997) 8221–8229.
[24] I. Dmitriev, V. Krasnykh, C.R. Miller, M. Wang, E. Kashentseva, G. Mikheeva, N. Belousova, D.T. Curiel, An adenovirus vector with genetically modified fibers demonstrates expanded tropism via utilization of a coxsackievirus and adenovirus receptor-independent cell entry mechanism, J. Virol. 72 (1998) 9706–9713.
[25] V. Krasnykh, I. Dmitriev, G. Mikheeva, C.R. Miller, N. Belousova, D.T. Curiel, Characterization of an adenovirus vector containing a heterologous peptide epitope in the HI loop of the fiber knob, J. Virol. 72 (1998) 1844–1852.
[26] H. Mizuguchi, N. Koizumi, T. Hosono, N. Utoguchi, Y. Watanabe, M.A. Kay, T. Hayakawa, A simplified system for constructing recombinant adenoviral vectors containing heterologous peptides in the HI loop of their fiber knob, Gene Ther. 8 (2001) 730–735.
[27] N. Koizumi, H. Mizuguchi, N. Utoguchi, Y. Watanabe, T. Hayakawa, Generation of fiber-modified adenovirus vectors containing heterologous

peptides in both the HI loop and C terminus of the fiber knob, J. Gene Med. 5 (2003) 267–276.
[28] H. Mizuguchi, T. Sasaki, K. Kawabata, F. Sakurai, T. Hayakawa, Fiber-modified adenovirus vectors mediate efficient gene transfer into undifferentiated and adipogenic-differentiated human mesenchymal stem cells, Biochem. Biophys. Res. Commun. 332 (2005) 1101–1106.
[29] M. Ito, M. Kodama, M. Masuko, M. Yamaura, K. Fuse, Y. Uesugi, S. Hirono, Y. Okura, I. Kato, Y. Hotta, T. Honda, R. Kuwano, Y. Aizawa, Expression of coxsackievirus and adenovirus receptor in hearts of rats with experimental autoimmune myocarditis, Circ. Res. 86 (2000) 275–280.
[30] Z. Li, R.V. Sharma, D. Duan, R.L. Davisson, Adenovirus-mediated gene transfer to adult mouse cardiomyocytes is selectively influenced by culture medium, J. Gene Med. 5 (2003) 765–772.
[31] H. Wayland, Microcirculation in pancreatic function, Microsc. Res. Tech. 37 (1997) 418–433.
[32] L. Jansson, P.O. Carlsson, Graft vascular function after transplantation of pancreatic islets, Diabetologia 45 (2002) 749–763.
[33] S.E. Raper, R.P. DeMatteo, Adenovirus-mediated in vivo gene transfer and expression in normal rat pancreas, Pancreas 12 (1996) 401–410.
[34] H. Taniguchi, E. Yamato, F. Tashiro, H. Ikegami, T. Ogihara, J. Miyazaki, β-cell neogenesis induced by adenovirus-mediated gene delivery of transcription factor pdx-1 into mouse pancreas, Gene Ther. 10 (2003) 15–23.
[35] E. Ayuso, M. Chillon, J. Agudo, V. Haurigot, A. Bosch, A. Carretero, P.J. Otaegui, F. Bosch, In vivo gene transfer to pancreatic beta cells by systemic delivery of adenoviral vectors, Hum. Gene Ther. 15 (2004) 805–812.

European Journal of Neuroscience, Vol. 25, pp. 2349–2363, 2007 doi:10.1111/j.1460-9568.2007.05499.x

Disruption of Kir6.2-containing ATP-sensitive potassium channels impairs maintenance of hypoxic gasping in mice

Akari Miyake,[1,*] Katsuya Yamada,[1,2,5,*] Tomohiro Kosaka,[1] Takashi Miki,[3] Susumu Seino[3] and Nobuya Inagaki[1,4,5]
[1]Department of Physiology, Akita University School of Medicine, Akita, Japan
[2]Department of Physiology, Hirosaki University School of Medicine, Aomori, Japan
[3]Division of Cellular and Molecular Medicine, Kobe University Graduate School of Medicine, Kobe, Japan
[4]Department of Diabetes and Clinical Nutrition, Kyoto University Graduate School of Medicine, 54 Kawahara-cho, Shogoin, Sakyo-ku, Kyoto 606-8577, Japan
[5]CREST of Japan Science and Technology Agency, Kawaguchi, Saitama, Japan

Keywords: depression, hypoxia, ATP-sensitive potassium channel, sigh, tachypnea

Abstract

Hypoxic gasping emerges under severe hypoxia/ischemia in various species, exerting a life-protective role by assuring minimum ventilation even in loss of consciousness. However, the molecular basis of its generation and maintenance is not well understood. Here we found that mice lacking Kir6.2- but not Kir6.1-containing ATP-sensitive potassium (K_{ATP}) channels [knockout (KO) mice] exhibited few gasps when subjected to abrupt ischemia by decapitation, whereas wild-type mice all exhibited more than 10 gasps. Under anesthesia, wild-type mice initially responded to severe hypoxic insult with augmented breathing (tachypnea) accompanied by sighs and subsequent depression of respiratory frequency. Gasping then emerged and persisted stably (persistent gasping); if the hypoxia continued, several gasps with distinct patterns appeared (terminal gasping) before cessation of breathing. KO mice showed similar hypoxic responses but both depression and the two types of gasping were of much shorter duration than in wild-type mice. Moreover, in the unanesthetized condition, the onset of terminal gasping in KO mice, which was always earlier than in wild-type mice, was unaltered by decreasing O_2 concentrations within the severe range (4.5–7.0%), whereas onset in wild-type mice became earlier in response to lowered O_2 concentrations. Thus, the mechanism responsible for regulating the hypoxic response in accordance with the severity of the hypoxia was dysfunctional in these KO mice, suggesting that Kir6.2-containing K_{ATP} channels are critically involved in the maintenance rather than the generation of hypoxic gasping and depression of respiratory frequency.

Introduction

Under severe hypoxia/ischemia, as in stroke and cardiac/pulmonary failure, reduced O_2 supply to the brain triggers a sequence of respiratory responses including an initial augmentation (tachypnea) followed by a depression of respiratory frequency and, if prolonged, electroencephalogram silence marking hypoxic coma. In this state, gasping, a spontaneous respiratory activity, can emerge and thereby improve the blood oxygenation state and increase the recovery rate (St. John & Knuth, 1981; Sanocka *et al.*, 1992; Khurana & Thach, 1996; Fewell, 2005). Despite its critical importance in protection of life, the molecular basis underlying such gasping remains poorly understood.

ATP-sensitive potassium (K_{ATP}) channels (Noma, 1983) consisting of pore-forming Kir6.*x* and sulfonylurea receptor (SUR) subunits (Inagaki *et al.*, 1995, 1996) couple the intracellular metabolic state of cells to electrical activity at the plasma membrane (Ashcroft, 1988; Seino, 1999). K_{ATP} channels are expressed in brain in various nuclei including brainstem (Mourre *et al.*, 1989; Mironov *et al.*, 1998) but their physiological role is only partially clear. We previously reported that mice lacking the Kir6.2 subunit of K_{ATP} channels [knockout (KO) mice] (Miki *et al.*, 1998) are extremely susceptible to generalized seizure after brief hypoxia (Yamada *et al.*, 2001). When subjected to severe hypoxia (~5% O_2), KO mice soon exhibited very low-voltage electroencephalogram, indicating loss of consciousness. Tonic convulsion then lasted for several seconds, after which generalized seizure was observed in the electroencephalogram, whereas in wild-type mice, medium to low-voltage waves predominated and gasping emerged after prolonged hypoxia. During the course of the study, we found that KO mice exhibited fewer gasps under hypoxia (unpublished observation), indicating involvement of the K_{ATP} channels in control of gasping.

Extensive studies on gasping have been reported (St. John & Knuth, 1981; Selle & Witten, 1941; Holowach-Thurston *et al.*, 1974; Khurana & Thach, 1996; Wang *et al.*, 1996; Ramirez *et al.*, 1998; Lieske *et al.*, 2000; Paton *et al.*, 2006). However, very different methods of inducing hypoxia have been used *in vivo* and *in vitro*, and characterizing gasping by the various methodologies is problematic (Ramirez & Lieske, 2003).

In the present study, we used three protocols to investigate the regulatory mechanism of hypoxic gasping in mice, including abrupt ischemia by decapitation and hypoxia in anesthetized and unanesthetized conditions. Differences in hypoxic responses between wild-type

Correspondence: Dr Nobuya Inagaki, [4]Department of Diabetes and Clinical Nutrition, as above.
E-mail: inagaki@metab.kuhp.kyoto-u.ac.jp

*A.M. and K.Y. contributed equally to this work.

Received 11 December 2006, revised 19 February 2007, accepted 22 February 2007

and Kir6.2 KO mice were investigated using methods including monitoring expiratory flow with a thermistor airflow sensor, respiratory body movement with a piezoelectric transducer (PZT) device (Sato *et al.*, 2006), expired O_2/CO_2 with a gas analyser and activity of the phrenic nerve. An experiment in unanesthetized condition was required because respiration under severe hypoxia is affected by both anesthesia level and body temperature (Fazekas *et al.*, 1941; Miller, 1949; Secher & Wilhjelm, 1968; Fewell, 2005), and could not be equalized among anesthetized mice subjected to phrenic nerve recordings. Mice exhibiting gasping were considered to be in a condition of hypoxic coma (loss of consciousness) based on electroencephalogram (Yamada *et al.*, 2001).

Materials and methods

Animals

Fifty-nine wild-type mice (C57BL/6J), 52 mice lacking Kir6.2-containing K_{ATP} channels (Miki *et al.*, 1998) and four Kir6.1-deficient mice (Miki *et al.*, 2002) were used in accordance with a protocol approved by the Akita University Institutional Committee for Animal Studies and followed the Akita University Guidelines for Animal Experimentation. The Kir6.2 and Kir6.1 genes were cloned from a 129/Sv mouse genomic DNA library. The mutant mice were backcrossed more than four times to C57BL/6 mice. All mice were adult males (>2 months). Urethane anesthesia (1.4 g/kg, i.p.) was used in all experiments under anesthetic condition. The anesthesia level was evaluated by monitoring respiration frequency and electrocardiogram. For the brief hypoxia experiment (see Results), the heart rate (652.6 ± 4.5/min, $n = 23$) and respiratory frequency before hypoxic challenge (4.0 ± 0.1 Hz, $n = 23$) of wild-type mice were not significantly different from those of KO mice (643.7 ± 7.1/min and 3.8 ± 0.1 Hz, respectively. $n = 12$). For the prolonged hypoxia experiment, the heart rate (628.7 ± 3.8/min, $n = 4$) and respiratory frequency before hypoxic challenge (4.0 ± 0.1 Hz, $n = 4$) of wild-type mice were not significantly different from those of KO mice (613.2 ± 14.8/min and 4.2 ± 0.2 Hz, respectively. $n = 5$).

Abrupt ischemia caused by decapitation

To compare central regulation of gasping of wild-type and KO mice in abrupt ischemia, the whole head was isolated by decapitation while the mouse was restrained on a PZT device, which converts mechanical motion into an electrical signal (PCT/JP03/01109; Sato *et al.*, 2006). The buffered PZT-produced signals were amplified by a custom-made amplifier (×1 or ×10), digitalized and filtered offline by commercially available software (CLAMPEX 8 and CLAMPFIT 8, Molecular Devices, Sunnyvale, CA, USA). To distinguish gasping from other body movements, respiration was simultaneously monitored by four infrared CCD cameras from different directions and stored on video tape or DVD. The number of gasps was counted from the stored image in reference to sharp deflections in the PZT-derived vibration signal. Gasps comprising double openings of the jaw (double or diphasic gasps) (Selle, 1944) were counted as two gasps in these experiments.

After dissection, brains were removed and fixed in 4% paraformaldehyde at 4 °C for later examination of the dissected portion of the spinal cord. Only cases of dissection caudal to the C2 level were analysed in the present study, as no gasp was seen when the dissection was made at the C0–C1 level in both wild-type and KO mice. Although we did not investigate this matter in the present study, it is possible that impairment of the C1 cell group has some role in the central regulation of respiration (Gang *et al.*, 1995).

Hypoxia experiments under anesthesia

Tracheotomy was performed in urethane-anesthetized mice. One end of a bent stainless steel cannula (6-mm-long, 18G flat-end needle) was inserted into the trachea and the open end was connected to a 2.5-mL open syringe (Fig. 1A). Care was taken to minimize the dead volume in the tracheal cannula and the tube connecting the cannula to the syringe. From the open end of the syringe, two Pharmed tubes (Saint-Gobain Performance Plastics, OH, USA) were inserted and fixed firmly to the syringe with a glue; one (thicker, internal diameter 2 mm) was for introducing hypoxic gas or air into the syringe and the other (thinner, internal diameter 1 mm) was set closer to the cannula end for effective sampling of the expired gas. The gas expired from the cannula, which was diluted to a certain extent by the atmosphere in the syringe, was continuously sampled (10 mL/min) and measured by an O_2/CO_2 analyser (1H-26, GE Healthcare, Tokyo, Japan).

In the syringe, changes in the temperature of outflow from the tracheal cannula were simultaneously monitored by a conventional thermistor-type airflow sensor (type 45257, GE Healthcare). To detect respiratory body movement, a PZT sensor, which was integrated into a heater plate for maintaining body temperature, was used (Sato *et al.*, 2006). As gasping is strongly affected by temperature (Fazekas *et al.*, 1941; Miller, 1949; Fewell, 2005), special care was taken to keep the rectal temperature under anesthesia at 37.0 ± 0.1 °C using a custom-made heater device, while also monitoring the surface temperature of the heater (Japanese Patent no. 3685983; Sato *et al.*, 2006). The rectal temperature was recorded with a thin thermistor probe 2 cm from the anus. Electrocardiogram was measured between the right forepaw and left hindpaw.

Two types of hypoxia experiments under anesthesia for either 60 s or a more prolonged period until cessation were conducted. Hypoxia was produced by switching the gas introduced into the syringe from room air to pre-mixed hypoxic gas with the same flow rate (500 mL/min) using microprocessor-controlled, electromagnetic three-way valves. The pre-mixed gas was produced from O_2 and N_2 gas by using mass flow meters (SEC-E40, HORIBA STEC, Kyoto,

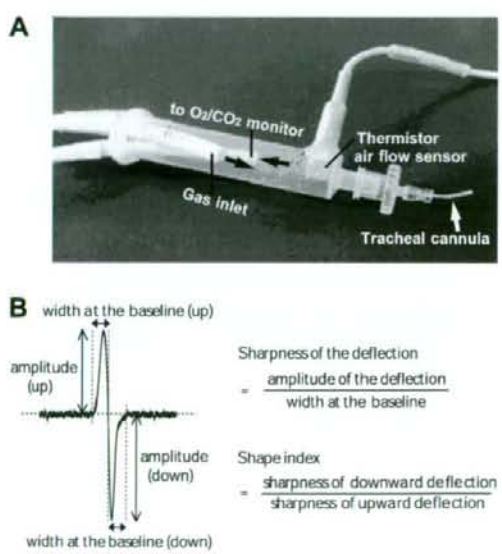

FIG. 1. Apparatus for introducing hypoxia to spontaneously breathing mouse in anesthetized condition (A) and piezoelectric transducer shape index (B).

Japan). When pre-mixed gas of 4.5–5.0% O_2 was introduced, the O_2 concentration within the syringe at 60 s after the opening of the valves was 5.0–5.5% (~16 s were needed for the atmosphere in the syringe to reach 5.5% O_2 for a pre-mixed value of 4.5% O_2). Thus, in the 60-s brief hypoxia experiment, the O_2 concentration was expressed as the value at 60 s after valve opening. In the prolonged hypoxia experiment, although the O_2 concentration reached closer to the pre-mixed value, the concentration at 60 s after the valve opening was also used to indicate the value.

In all of the prolonged hypoxia experiments and in some of the 60-s brief hypoxia experiments, the right phrenic nerve was identified and unsheathed. Nerve activity was recorded with bipolar silver electrodes (diameter 0.1 mm, interpolar distance unfixed), amplified (time constant 0.3 ms, cut-off frequency of low-pass filter 1 kHz; Bioelectric Amplifier 4124, GE Healthcare) and stored in a PC (see Digitalization section below).

Tachypnea, sigh and depression frequency in anesthetized condition

The onset of tachypnea was marked as the time point at which the ratio of the respiratory frequency under hypoxia relative to the mean frequency before hypoxia (0–10 s) continuously exceeded 100%, except for a possible single fluctuation.

Sigh was characterized by a large inspiration followed by an extraordinarily large-amplitude expiration and a brief post-sigh apneic period (Nakamura *et al.*, 2003). The magnitude of the expiration could be detected by a large upward deflection in the traces of expired CO_2 as well as by the thermistor airflow sensor. The upward deflection in the thermistor trace was followed by a wide and deep downward deflection, which was clearly distinguished from those of neighboring large breaths in the brief hypoxia experiment (see Results). The shape of the downward deflection of sigh reflects both the amplitude and width of the preceding upward deflection, the amplitude of the downward deflection becoming larger as the width of the upward deflection becomes wider according to the time constant of an AC amplifier (0.3 s) and software high-pass filter (> 1 Hz). In addition, the presence of the post-sigh apneic period also affected the shape of the downward deflection. A similar consideration is also applicable in discrimination of terminal gasping and persistent gasping in the prolonged hypoxia experiment (see Results).

The onset of depression was defined as the time point at which the ratio of the respiratory frequency under hypoxia relative to the mean frequency before hypoxia fell below 100%. The duration of depression was counted as the period from its onset to the beginning of persistent gasping (see next paragraph).

Shape index of piezoelectric transducer response under anesthesia

In the anesthetized condition, both inspiratory and expiratory body movement can be detected directly as vertical motion by the PZT device placed under the body (Sato *et al.*, 2006). The PZT device was moveable, and was set in the position at which the upward and downward deflections of the PZT signal corresponded to inspiratory and expiratory body movement, respectively, which was confirmed by simultaneously monitored changes in the phrenic nerve discharge, expiratory CO_2 and airflow in the outlet of the tracheal cannula. Under urethane anesthesia, respiratory body movement detected by PZT showed a biphasic shape. Evaluation of the symmetry of the upward and downward deflections in PZT shape was accomplished as follows (Fig. 1B). To measure the sharpness of the deflection, the amplitude was divided by its width at the baseline. The ratio of the sharpness of the downward deflection to the sharpness of the upward deflection is the shape index, which is 1 when the shapes of the upward and downward deflections are symmetrical.

Hypoxia under unanesthetized condition

Individual mice were subjected to hypoxia while held in a conical skirted, tapered centrifuge tube (internal diameter 25–27 mm, no. 62.559, Sarstedt, Numbrecht, Germany) with mouth and nose protruding slightly from the opening (diameter 4.5 mm) in the bottom of the tube for breathing gas introduced from the inlet (Fig. 2). The dead volume outside the hole was minimized with silicon filling. The dead volume within the tube was decreased by a soft rubber inner plug, the position of which was adjusted to minimize disturbances of natural respiration. Expired gas from the centrifuge tube was monitored by an O_2/CO_2 analyser. A very slow flow rate (75 mL/min) for introducing pre-mixed gas (O_2 ranging from 4.5 to 7.0% or air for control) was selected to detect gasping while minimizing seizure. At this flow rate, individual expiratory breaths during gasping could be detected by sharp deflections in the sampled CO_2 trace. When the mouse breathed room air, the O_2 concentration in the sampled expired gas was slightly lower and the CO_2 concentration was higher due to the slow flow rate.

The whole centrifuge tube was placed on the PZT device. The respiratory body movement of the mouse caused a small vibration of the rubber plug (Fig. 2) and a drift of the center of gravity of the centrifuge tube. The resulting angular moment of the tube was transferred to the PZT device as vertical motion. Inspiratory body movement produced downward deflections of the PZT signal in the resting eupneic condition. Thus, the respiratory frequency in the unanesthetized condition could be measured by PZT deflections while being confirmed by percentage CO_2 changes except when large body movements overlapped.

The onset of tachypnea in unanesthetized condition was determined as the time point at which the extrapolated rising phase of the relative respiratory frequency in tachypnea intersected the 100% line (mean respiratory frequency before hypoxic challenge) (see Fig. 11A2 and B2). The onset of depression subsequent to tachypnea was similarly determined but by using the falling phase in tachypnea. The onset of terminal gasping was determined as the time point at which the duration between positive and negative PZT deflections abruptly became wide during the period before cessation. Precise determination of the duration of terminal gasping in unanesthetized condition was difficult because the convulsive movements just before cessation also produced deflections in the PZT signal and an increase in CO_2.

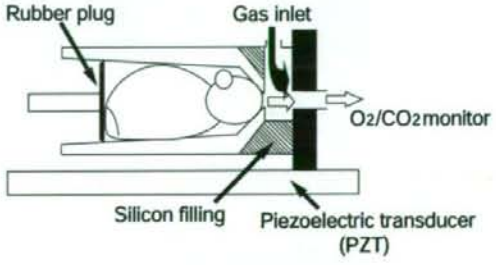

FIG. 2. Apparatus for introducing hypoxia to mouse in unanesthetized condition. PZT, piezoelectric transducer.

Digitalization

All bioelectric signals, including PZT-derived signals, were digitized at a sampling rate of 2 kHz (CLAMPEX 8, Molecular Devices) in anesthetized conditions and stored in a PC. A low sampling rate (1 kHz) was used for hypoxia experiments under unanesthetized condition. A software high-pass filter (cut-off 1 Hz, CLAMPfiT 8) was used to analyse electrocardiogram, thermistor airflow sensor signal and phrenic nerve activity. A low-pass filter (cut-off 500Hz) was used for CO_2 monitoring.

Statistical analysis

Values were expressed as mean ± SE. Statistical comparison was made by unpaired or paired *t*-test using commercially available software (STATVIEW 5.0, SAS Institute, Cary, NC, USA).

Results

Gasping of knockout and wild-type mice following decapitation

In the normoxic condition, the respiratory frequency of awake Kir6.2 KO mice (3.4 ± 0.3 Hz, body weight 27.1 ± 0.4 g, $n = 10$) was not significantly different from that of wild-type mice (3.2 ± 0.2 Hz, body weight 26.5 ± 0.4 g, $n = 12$). However, when subjected to abrupt ischemia by decapitation, all wild-type mice exhibited more than 10 gasps, whereas only a very few gasps were detected in the KO mice and nine out of 20 KO mice showed no gasping at all (Fig. 3A–C). In addition to the significant difference in the number of gasps, the duration of gasping was considerably shorter in KO than in wild-type mice (Fig. 3D). In contrast, mice lacking the K_{ATP} channel subunit Kir6.1 (vascular smooth muscle-type K_{ATP} channels) exhibited gasps numbering 12.8 ± 0.3 ($n = 4$) with a duration of 17.3 ± 0.5 s ($n = 4$), not significantly different from that of wild-type mice, suggesting involvement of Kir6.2-containing K_{ATP} channels in central regulation of gasping.

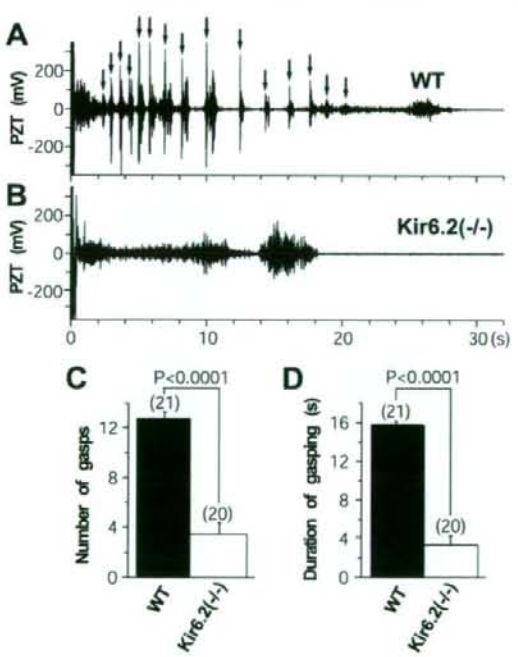

FIG. 3. Gasping caused by decapitation in wild-type (WT) and knockout (KO) mice. (A) Movement of WT head detected by piezoelectric transducer (PZT) sensor after decapitation (0 s). Arrows indicate gasping verified by video recordings (see Materials and methods). (B) Similar to A but of a KO mouse. The initial vibrations detected before 1 s after the isolation were caused by contact of the head with the PZT sensor. During this period, no gasp was observed in all mice tested. Comparison of the number (C) and total duration (D) of gasping between WT and KO mice.

Respiratory changes induced by brief hypoxia in anesthetized condition

Tachypnea and sighs

To further investigate the relevance of K_{ATP} channels in hypoxic gasping, spontaneously breathing mice were subjected under anesthesia to rapidly introduced, severe hypoxia for 60 s. This period was chosen so that both types of mice could revive after re-exposure to normoxia in the anesthetized condition. The O_2 concentration imposed on mice (5.0–5.5% measured at 60 s after introduction) was selected based on our previous study (Yamada *et al.*, 2001).

Three indices reflecting respiration were measured: changes in O_2/CO_2 concentration within the syringe connected to the tracheal cannula, changes in temperature fluctuation due to expiratory flow and respiratory body movement (Fig. 1A, see Materials and methods). Phrenic nerve activity was also monitored in some cases. However, it is known that respiratory responses to severe hypoxia are extremely sensitive to the anesthesia level and body temperature (Secher & Wilhjelm, 1968; Fewell, 2005), and the anesthesia levels of the mice subjected to phrenic nerve recordings were difficult to keep equalized during the hypoxia experiment. Accordingly, traces of phrenic nerve recordings were selected to represent typical hypoxic responses (Fig. 4A and B).

The initial responses of wild-type mice, along with a rapidly declining O_2 concentration, were augmented respiratory frequency (tachypnea, Fig. 4, A1 and A2, onset indicated by open arrowhead) and a subsequent extraordinarily large breath (asterisks in Fig. 4, A1). The large breath, referred to as a sigh, was easily identified by its biphasic large deflection in the trace of the thermistor airflow sensor. As indicated by the concomitant increase in expired CO_2 (Figs 4, A1, and 5, A1), these deflections reflect the large-amplitude expiration of a sigh (see later sections for details).

The onset of tachypnea and initial sigh were similar in wild-type and KO mice (Figs 4, A1–C1, and 6, A1 and B1). However, the maximal respiratory frequency during tachypnea was higher and the peak period of tachypnea (from onset to maximum tachypnea) was longer in KO than in wild-type mice (Figs 4, A2–C2, 5, A1 and B1, and 6, A2 and A3). In addition, most (10/12) KO mice exhibited an apnea-like period (duration 13.3 ± 1.4 s, onset 26.9 ± 1.0 s, $n = 10$) following tachypnea (Figs 4, C1 and C2, and 5C). During this apnea-like period, the respiratory frequency may have been too high, as indicated by the PZT deflections, for these breaths to be detected by thermistor or CO_2 sensor (Fig. 5C). Accordingly, the apnea-like periods were not counted as depression in the anesthetized experiment. No such apnea-like period was detected in the wild-type mice tested ($n = 23$) during the 60-s hypoxic period.

Depression in respiratory frequency

Following the tachypnea, the respiratory frequency of wild-type mice was quickly depressed to a value below the mean frequency before hypoxia (depression, after filled arrow in Fig. 4, A2). In addition, the amplitude of CO_2 and thermistor airflow sensor traces progressively

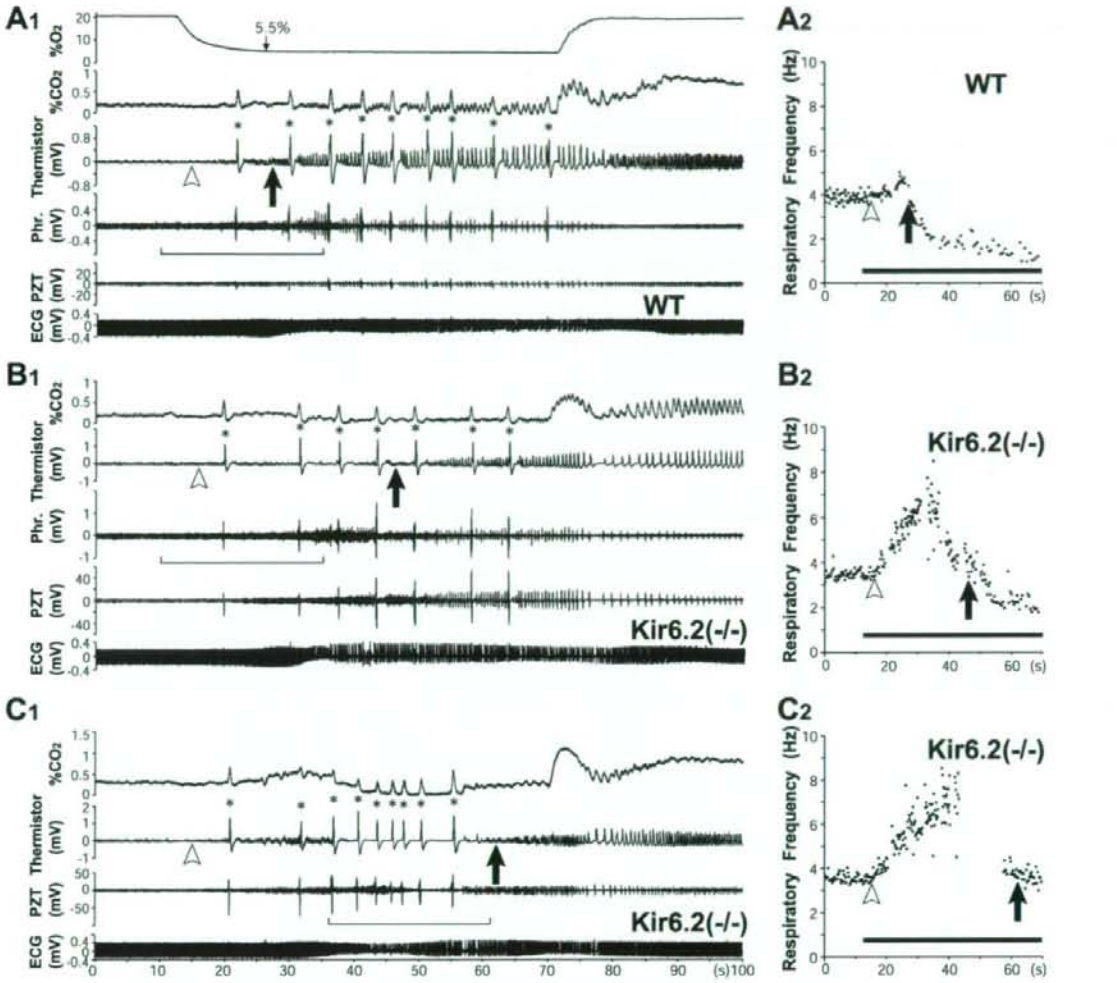

FIG. 4. Brief hypoxia (60 s)-induced respiration changes in mice under anesthesia. (A1) Representative responses of a wild-type (WT) mouse. Electromagnetic three-way valve for introducing hypoxic gas was opened at 10 s (the time lag in percentage O_2 change was due to dead volume in the gas inlet tube and syringe). At 60 s after valve opening, percentage O_2 in the syringe reached 5.0% (the time at 5.5% O_2 is indicated). Delay originating from the response time of the O_2/CO_2 gas analyser (~7.5 s) was corrected. An increase in percentage CO_2 reflects expiratory outflow from the tracheal cannula. Temperature increase due to expiratory flow was monitored by a thermistor airflow sensor (Thermistor; see Materials and methods). Biphasic large deflections in the trace of the thermistor (asterisks) are referred to as 'sighs'. Onsets of tachypnea and depression are indicated by open arrowhead and filled arrow, respectively. Operation for phrenic nerve recording (Phr.) in this mouse minimally affected the response. Inspiratory and expiratory body movement were monitored by piezoelectric transducer (PZT) deflections in the opposite direction. Electrocardiogram (ECG) was monitored. The underlined period is expanded in Fig. 5A to show details in the initial hypoxic responses. (B1) Similar to A1 but of a knockout (KO) mouse. (C1) Similar to B1 but of another KO mouse showing apnea-like period interrupted by sighs. Phrenic recording was not conducted in this case. Detail in the responses during the apnea-like period (underlined) is shown in Fig. 5C. (A2) Change in respiratory frequency of WT mouse shown in A1. Filled bar denotes period of actual hypoxic challenge. Open arrowhead and filled arrow indicate the onset of tachypnea and depression, respectively (see Materials and methods). (B2 and C2) Similar to A2 but of KO mice shown in B1 and C1, respectively. In the brief hypoxia experiment, thermistor sensor responses were used to count frequency and sighs were not counted. Hence, the trace in C2 shows an intermittent period after tachypnea.

increased, indicating increased tidal volume during depression (Figs 4, A1, and 5, A1). The frequency slowed further to below 2 Hz in a short period, while a large tidal volume was maintained (Figs 4, A1 and A2, and 5, A1). Based only on the tidal volume and interbreath interval, the slow respiration during this period (frequency $<\sim$2Hz) may be regarded as gasping. With regard to phrenic nerve activity, the burst of gasping in small animals such as mice has been characterized by its larger amplitude and shorter duration compared with those in eupnea, in addition to a long intergasp interval (St. John & Paton, 2003). However, the amplitude of the phrenic bursts in wild-type mice during this slow respiration period was frequently not much larger (Fig. 4, A1, see the trace of phrenic activity) than that during eupnea and the duration of the burst was long in some instances (see also Fig. 8, A2), making it difficult to determine if such slow respiration is gasping or depression.

Although KO mice also showed a depression similar to that seen in wild-type mice, its onset was significantly delayed (Figs 4B and C, and 6C). Thus, tachypnea was more quickly depressed in wild-type

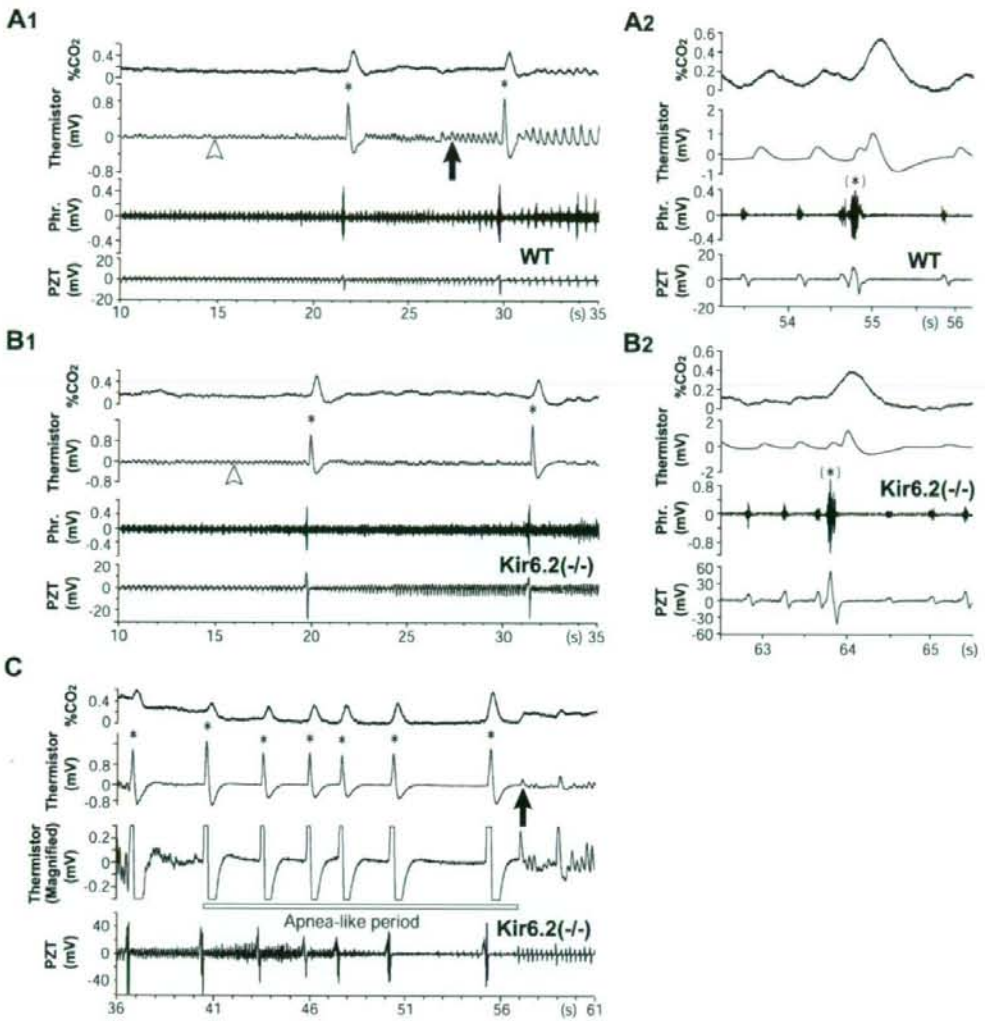

FIG. 5. Details in respiratory responses during brief hypoxia. (A1) Initial hypoxic responses of a wild-type (WT) mouse underlined in Fig. 4A1. Onsets of tachypnea (open arrowhead) and depression (filled arrow) are indicated in the thermistor trace. Asterisks denote sighs (as in Fig 4). (B1) Similar to A1 but of a knockout (KO) mouse underlined in Fig. 4B1. (A2 and B2) Phrenic nerve discharges corresponding to sighs (asterisks in parenthesis) of WT and KO mice in A1 and B1, respectively. To show the phrenic discharge pattern, these sighs were chosen from the later period when sighs emerged independently of neighboring breaths, as the initial sighs in A1 and B1 during tachypnea overlapped to a variable extent with neighboring fast breaths. Simultaneous recordings of phrenic nerve activity and piezoelectric transducer (PZT) responses demonstrate that the upward deflection in the PZT trace correlated well with the phrenic burst, i.e. the inspiratory activity. The response time-lag in percentage CO_2 was corrected as in Fig. 4. As other traces are shown in real time, the thermistor responses are shown slightly delayed from phrenic discharges and PZT responses. (C) Details in apnea-like period after tachypnea underlined in Fig. 4C1. The thermistor response in the second trace is redrawn in the third trace at a magnified scale to demonstrate that breaths between sighs were undetectable by the thermistor sensor. As the PZT sensor is extremely sensitive, very fast breathing-like motions were detected between sighs in the initial stage of the apnea-like period. Phr., phrenic nerve recording.

than in KO mice in the anesthetized condition. A similar further slowing of respiration (< 2 Hz) was also observed in some KO mice within the brief hypoxic period (Fig. 4, B2).

Characterization of sighs during brief hypoxia

The extraordinary large-amplitude breaths termed here as sighs are characterized by phrenic nerve discharge with an amplitude much larger than that of a eupneic breath (Fig. 4, see also Fig. 5, A2 and B2). In addition, a sigh was clearly distinguishable from neighboring breaths by the deeper and wider downward deflections seen in the trace of the thermistor airflow sensor (Fig. 4A–C), indicating that sighs involve expiration of larger amplitude and longer duration (see Materials and methods). In addition, sighs emerged independently of the neighboring breaths (Fig. 5, A2 and B2, asterisks) and were followed by a short duration post-sigh apneic period (Nakamura *et al.*, 2003).

When the number of sighs was counted on this definition, the onset and number of sighs were similar in wild-type and KO mice, except

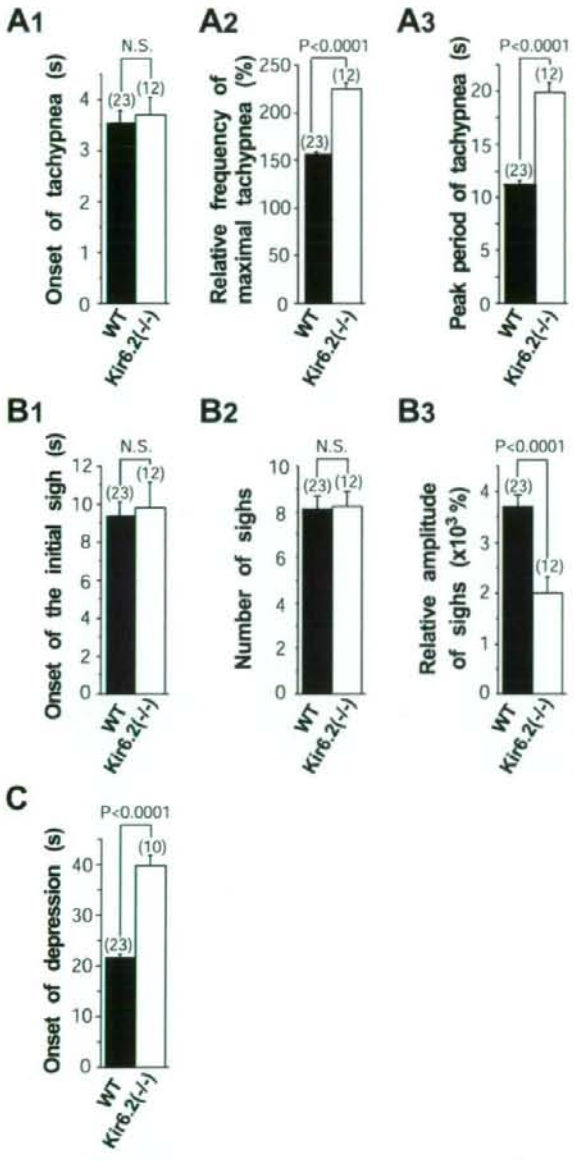

FIG. 6. Comparison of brief hypoxia-induced respiratory changes between wild-type (WT) and knockout (KO) mice. (A1, A2 and A3) The onset, maximal respiratory frequency relative to the mean frequency before hypoxic challenge and peak period (time from onset to maximum) of tachypnea, respectively. (B1 and B2) Onset and the number of sighs. (B3) The mean amplitude of sighs relative to that of breaths before hypoxic challenge evaluated by thermistor sensor. (C) Onset of depression. Two KO mice did not show depression during the 60-s hypoxic period. Onsets in all figures were measured from the time that the O_2 concentration actually began to decrease (see Fig. 4A1). N.S., not significant.

that the mean amplitude of sighs relative to that of eupneic breaths was lower in KO than in wild-type mice (Fig. 6, B1–B3). These results suggest that K_{ATP} channels are not required in the generation and maintenance of sighs.

Respiratory changes in prolonged hypoxia in anesthetized condition

The brief hypoxia experiment suggested investigation of respiratory changes during a longer hypoxic period. We then examined the effect of prolonged hypoxia in the anesthetized condition while recording phrenic nerve activity, introduced as in the brief hypoxia experiment (to 5.0% O_2 in 60 s) and maintained until cessation. As the hypoxic period was longer, the O_2 concentration finally reached nearly the value of the pre-mixed gas (4.5% O_2) (see Materials and methods).

In wild-type mice, tachypnea, sighs and depression were elicited during the initial 60-s hypoxia in a manner essentially similar to that described in previous sections (Figs 7 and 10A). However, after this period, the sighs ceased and the basal respiratory frequency became gradually slower, stabilizing at a very low frequency (< ~0.5 Hz), which persisted for tens of seconds (Figs 7A and 9, A1). The PZT signal during this stable phase exhibited a biphasic symmetrical shape (Fig. 8, A3, bottom trace), whereas in the eupneic period the shape was asymmetrical, with upward deflection of less amplitude and longer duration than the subsequent downward deflection (Fig. 8, A1). In the depression period preceding this stable phase, the PZT signal also exhibited an asymmetrical shape in the beginning but gradually shifted to symmetrical (Figs 7A, and 8, A2 and A3). To quantify the symmetry of the PZT shape, we used a shape index in the present study that becomes closer to 1 as the PZT shape becomes more symmetrical (see Materials and methods).

As shown in Fig. 9, B1, the shape index during the initial phase of depression in wild-type mice fluctuated greatly but the value soon became stable at a value close to 1. The shape index clearly shows a stable respiration phase of some duration after the onset of depression (open arrow in Fig. 9, B1). From this point, respiratory body movement detected by PZT shifted to biphasic symmetrical, reflecting an inspiration followed by an expiration involving an almost equal amount of vertical motion. Thus, a PZT shape index that became stable at a value close to 1 (ranging from 0.4 to 2.0) was termed persistent gasping. The duration of the depression in respiratory frequency was then counted as the period from its onset (filled arrow in Fig. 9, A1, when the respiratory frequency after tachypnea first decreased to a value less than the mean frequency before hypoxia) until the onset of persistent gasping (open arrow in Fig. 9, B1).

After the onset of depression (filled arrow in Fig. 9, A1), the width of the phrenic burst also decreased gradually in wild-type mice (Fig. 9, C1) but some fluctuation was still seen. In contrast, during persistent gasping, the phrenic burst showed a stable value that was significantly shorter (0.06 ± 0.00 s, $n = 4$) than during eupnea (0.11 ± 0.09 s, $n = 4$, $P < 0.005$, paired t-test; Figs 8, A1 and A3, and 9, C1), indicating that breathing during persistent gasping meets at least one of the conventional criteria of gasping, a shorter duration of phrenic burst than in eupnea, although the amplitude of the burst was not always much larger than in eupnea (see also Fig. 7A).

In KO mice, depression in respiratory frequency could be detected (Figs 7B, 8B and 9, A2) but its onset was delayed by ~15 s and its duration was shorter by ~80 s than in wild-type mice (Fig. 10A, see also Fig. 6C). As a consequence, the onset of persistent gasping in KO mice was significantly earlier than in wild-type mice (Figs 9, B1 and B2, and 10, B1).

When the hypoxic condition was continued further, the stable period of persistent gasping in wild-type mice stopped abruptly with a dramatic increase in the width of the phrenic burst, whereupon respiration ceased (Figs 7A and 8, A4; after thin arrow in Fig. 9, C1). The mean width of the phrenic bursts of the last four gasps except for the very last one of the terminal breaths was significantly wider

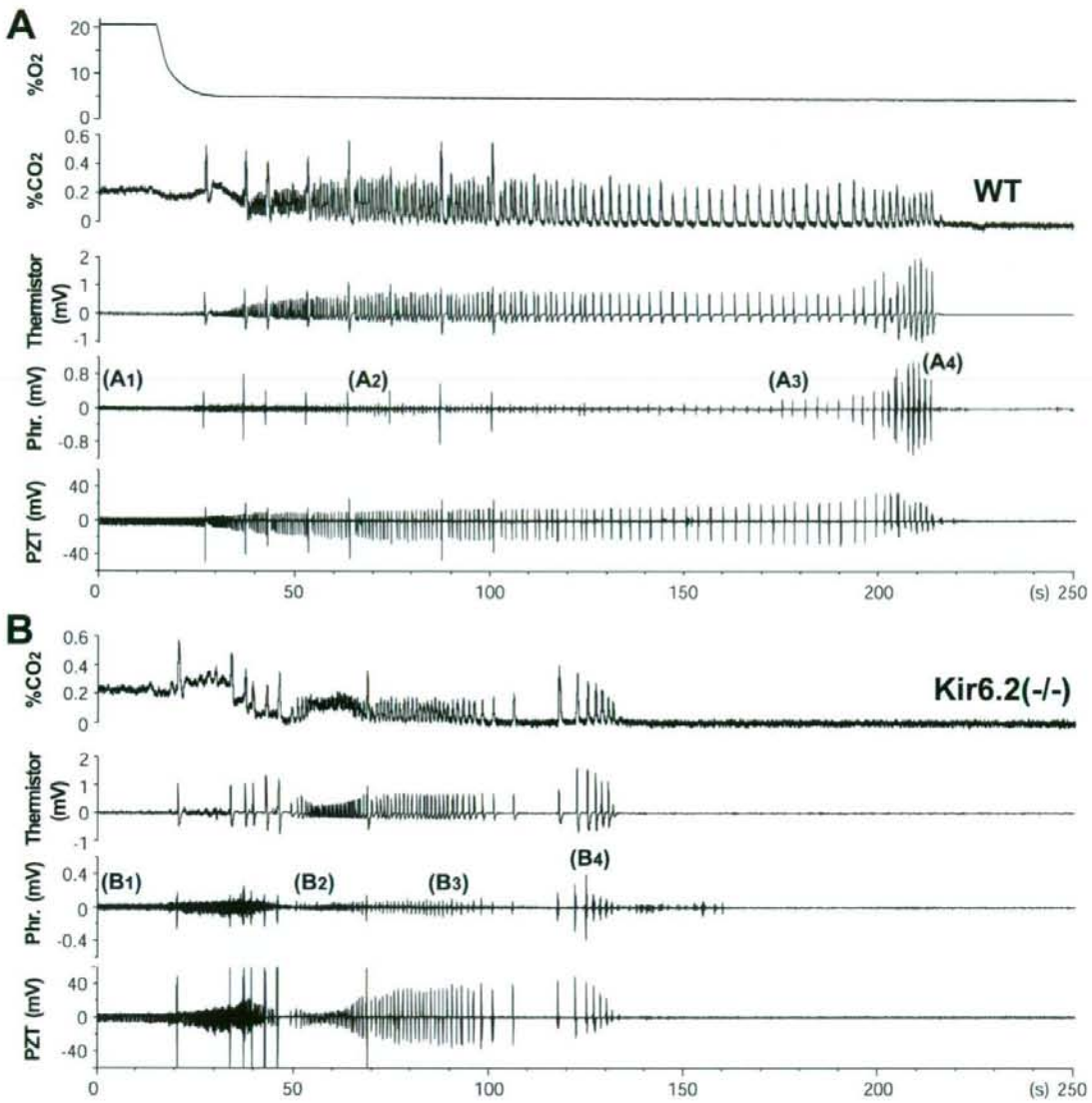

FIG. 7. Changes in respiration of wild-type (WT) (A) and knockout (KO) (B) mice subjected to hypoxia in a similar manner to the brief hypoxia (5.0% O_2 at 60 s) in anesthetized condition but for a more prolonged period. (A) Following the initial 60 s from hypoxia onset, stable, very slow respiration persisted until the emergence of several terminal breaths of large expiratory flow similar to the sighs seen in the thermistor trace but exhibiting a much wider phrenic burst than that of sighs. (B) Similar to A but of a KO mouse. Apnea-like periods are seen after tachypnea and before the terminal breaths. Responses marked by A1–4 and B1–4 in parenthesis are shown magnified in Fig. 8.

(0.33 ± 0.02 s, $n = 4$) than that of phrenic bursts during persistent gasping (0.06 ± 0.00 s, $n = 4$; $P < 0.005$, paired t-test). Thus, breathing after the time point at which the width of the phrenic burst showed an abrupt increase (thin arrow in Fig. 9, C1) was termed terminal gasping and persistent gasping continued until the onset of terminal gasping in the anesthetized experiment.

Corresponding to the large width of phrenic bursts in terminal gasping, which indicates a large inspiration, the duration between positive and negative PZT deflections was long, i.e. movement during expiration showed a delayed peak (Fig. 8, A4, downward deflections in the bottom trace). Indeed, the time point at which the width of the phrenic burst began to increase (Fig. 9, C1, thin arrow) correlated well with the shape index of the PZT falling close to 0 (Fig. 9, B1 and C1), reflecting an increase in the duration of individual expiratory flow, especially very close to the baseline (Fig. 8, A4). In addition, the amplitude of the downward deflections in the trace of the thermistor airflow sensor during terminal gasping was as large as that of sighs (Fig. 7A, third trace), also suggesting a long duration and large amplitude expiratory breath of terminal gasping as mentioned in the analysis of sighs above. The long duration of the individual expirations was most clearly seen in the PZT traces in some wild-type and KO mice (Fig. 8, B4, bottom trace).

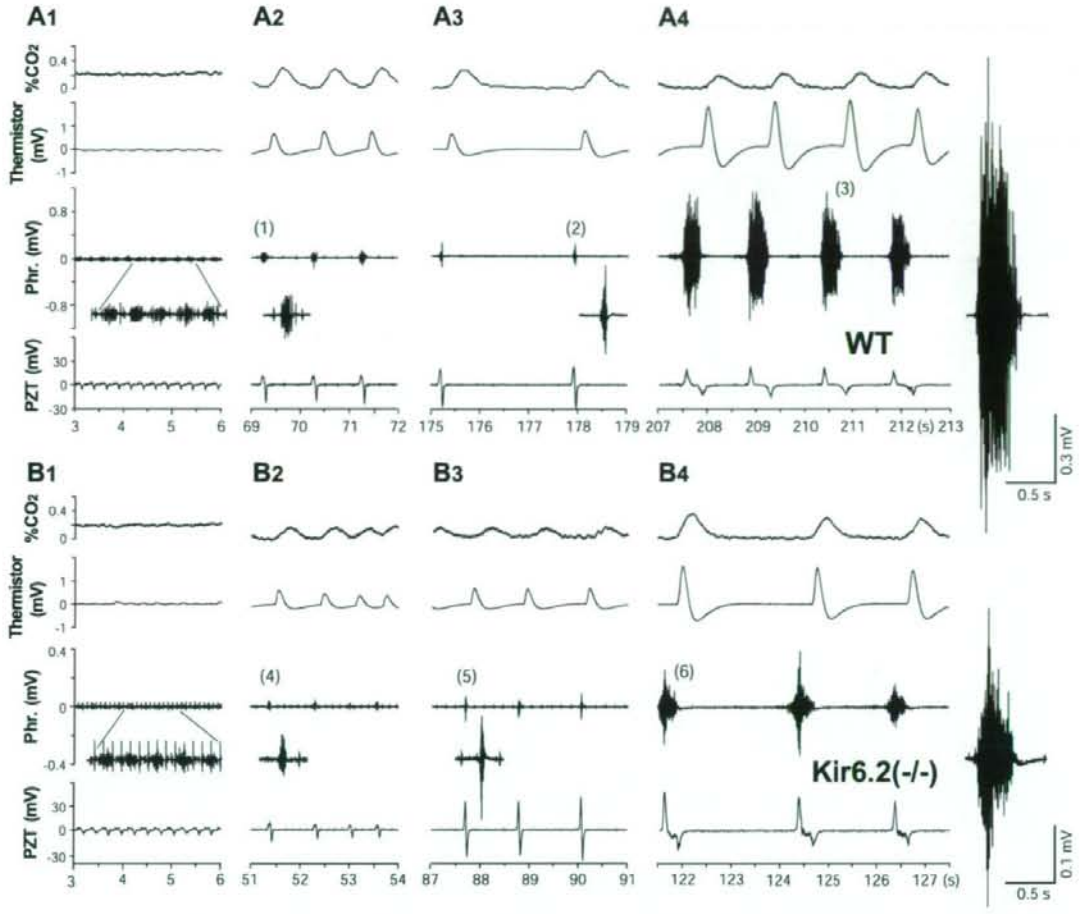

FIG. 8. Details of respiratory responses of wild-type (WT) (A) and knockout (KO) (B) mice during prolonged hypoxia at time points marked in Fig. 7. (A1) Control breaths before hypoxic challenge. The third trace represents phrenic nerve discharges. Note that the piezoelectric transducer (PZT) responses show asymmetrical shape. (A2) Typical traces during depression. The amplitude of percentage CO_2 and thermistor response was greatly increased. Responses numbered above are enlarged in insets. Note that PZT responses show asymmetrical shape during depression. The upward PZT deflection of wide duration and intermediate amplitude correlates well with the phrenic discharge above. (A3) A typical example of breaths during the stable, slow respiration, characterized by short width, relatively large amplitude phrenic discharge and PZT response of biphasic symmetrical shape. (A4) Terminal breaths characterized by phrenic discharge are much wider than other breaths and have extremely large amplitude. The shape of PZT response of terminal breaths is distinct from others during the preceding hypoxic period. Ordinates shown in A1 are common to A2–4. Scales for the phrenic discharge in the rightmost inset are common to other insets in A. (B1–4) Similar to A1–4 but of a KO mouse. Phr., phrenic nerve recording; PZT, piezoelectric transducer.

In KO mice, both the duration of depression and persistent gasping were much shorter than in wild-type mice (Figs 9, B2 and C2, and 10, A2 and B2), and the onset of terminal gasping was significantly earlier than in wild-type mice (Figs 9, C2, and 10, C1). The duration of terminal gasping was also significantly shorter in KO than in wild-type mice (Fig. 10, C2), indicating a crucial role of the K_{ATP} channels in the maintenance of depression and persistent and terminal gasping in the anesthetized condition.

Hypoxia-induced respiratory changes in unanesthetized condition

Hypoxic responses were also analysed under unanesthetized condition to exclude the influence of anesthesia. In preliminary tests, all wild-type and half of the KO mice exhibited no gasps at 8–9% O_2 within the recording period (1500 s). Below 4% O_2, or if the hypoxia was introduced as rapidly as in the anesthetized experiments, generalized convulsive seizure interfered with the detection of gasping in KO mice (Yamada *et al.*, 2001). Thus, the experiments were performed at O_2 concentrations from 4.5 to 7.0% at a very slowly declining rate of O_2 while CO_2 changes and body movement were monitored (see Materials and methods).

In these conditions, changes in the respiratory frequency could readily be detected by the PZT responses (see Materials and methods), the shapes of which were essentially similar to those detected in anesthetized condition (Fig. 11, A1 and B1). Tachypnea (onset, open arrowhead in Fig. 11, A2 and B2) and subsequent depression (onset, filled arrow in Fig. 11, A2 and B2) were detected in both wild-type and KO mice. At 4.5–5.0% O_2, no significant difference in onset of tachypnea was detected between wild-type and KO mice, as in the

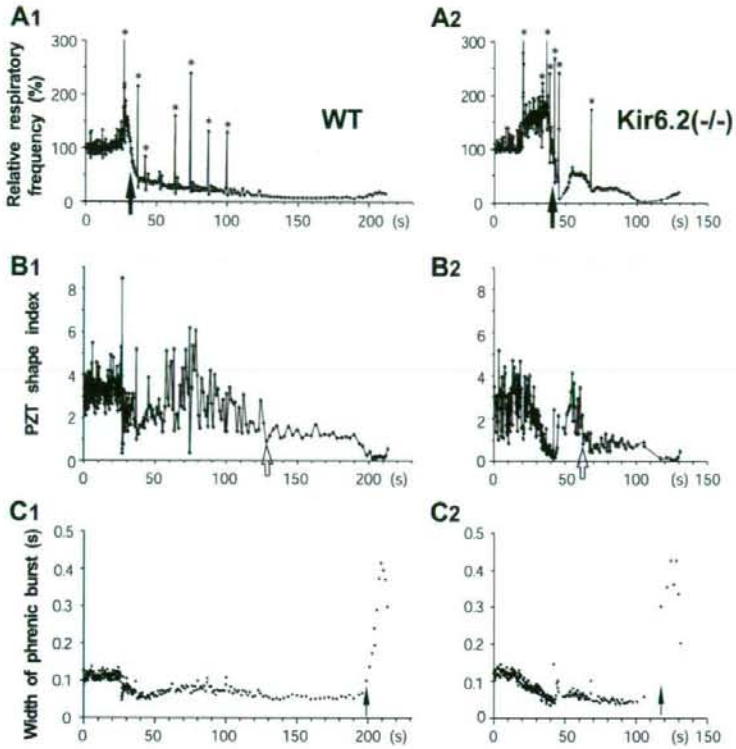

FIG. 9. Quantitative analyses of the respiratory responses of wild-type (WT) (A1, B1 and C1) and knockout (KO) (A2, B2 and C2) mice during prolonged hypoxia depicted in Fig. 7. Changes in the respiratory frequency relative to the mean frequency before hypoxic challenge (0–10 s) of WT (A1) and KO (A2) mice. The onset of depression in KO mice (filled arrow in A2) was delayed compared with WT (filled arrow in A1). In these plots, respiratory frequency was counted by piezoelectric transducer (PZT) deflections with reference to expiratory flow. Asterisks indicate transient tachypnea around extraordinarily large breaths (sighs). (B1 and B2) Similar to A but changes in the PZT index, reflecting symmetry of the upward (inspiration) and downward (expiration) deflections of the PZT response. Open arrows indicate the time point at which the shape index shows a relatively constant value close to 1, i.e. the beginning of persistent gasping. For convenience, values in A and B (but not C) are connected by lines. (C1 and C2) Similar to A but changes in width of phrenic burst. An abrupt increase in the width is clear (thin arrows), suggesting that gasping of a distinct type begins (terminal gasping). Note the blank in the trace in C2, which indicates the apneic period before terminal gasping in KO mice.

anesthetized experiments (Fig. 12A). A similar correspondence was also detected in other concentration ranges (data not shown). In addition, unlike the anesthetized condition, no difference in peak period or maximal respiratory frequency of tachypnea ($P = 0.91$ and 0.58, respectively) was detected between wild-type ($n = 6$) and KO ($n = 4$) mice at 4.5–5.0% O_2, at which no significant difference in respiratory frequency was detected before hypoxic challenge. Consistently, the onset of depression that emerged after the tachypnea was also similar in the two types of mice (Fig. 12B).

One of the most distinctive features of the respiratory responses of wild-type mice in the unanesthetized condition was that the first half of the hypoxic period comprised irregularly mixed depressions of variable frequency (filled arrowheads in Fig. 11, A2) and apnea-like periods (open squares in Fig. 11, A2; very low amplitude in percentage CO_2 and PZT traces in Fig. 11, A1), frequently accompanied by large body movements (Fig. 11, A1, large deflections in PZT trace). Imprecise discrimination of depressions and apnea-like periods made evaluation of the total period of depression difficult; nevertheless, the responses could be discerned by changes in the respiratory frequency (Fig. 11, A2) and differences in the height of the percentage CO_2 trace in comparison with the PZT response (Fig. 11, A1). In fact, the duration of depression including the apnea-like period in wild-type mice (summation of the initial depression shown in Fig. 11, A2 with the periods indicated by filled arrowheads and open squares) was longer than in KO mice (estimated as in Fig. 11, B2).

Despite the irregularity in the hypoxic responses, a stable, slow respiration rhythm having a PZT shape distinct from that in the initial half of the hypoxic period eventually emerged in all wild-type mice tested [Fig. 11, A1, inset (1)]. This slow respiration exhibited a PZT response of either symmetrical biphasic [Fig. 11, A1, inset (1)] or triphasic [Fig. 11, A1, asterisk in inset (2)] shape and persisted until just before the terminal breaths [Fig. 11, A1, inset (3)]. The biphasic PZT shape was similar to that of the persistent gasping in anesthetized condition (Fig. 8, A3). However, the triphasic shape was produced by body movement possibly reflecting an expiration/inspiration/expiration sequence. As the biphasic and triphasic shapes emerged unpredictably during the hypoxic period, we included both types as persistent gasping in the present study.

The PZT shape of the terminal breaths in wild-type mice was similar to that in terminal gasping in anesthetized experiments, especially the long duration between positive and negative deflections [inset (3) in Fig. 11, A1; see also PZT trace in Fig. 8, A4], and in most cases a sharp deflection followed by a wide valley in the opposite direction. In addition, there was a clear tendency to a hypoxic response in accord

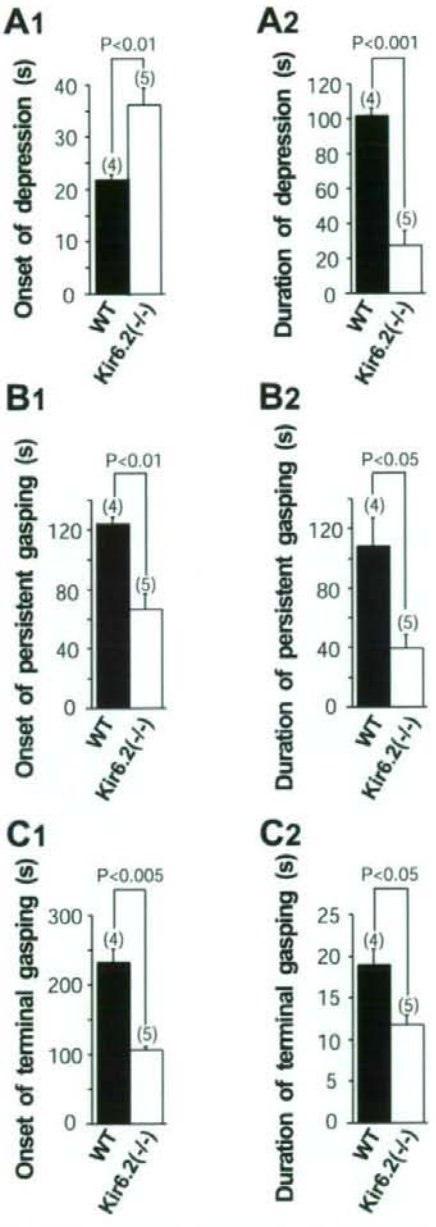

FIG. 10. Statistical comparison of depression (A), persistent gasping (B) and terminal gasping (C) under prolonged severe (5.0% O_2 at 60 s after valve opening) hypoxia between wild-type (WT) and knockout (KO) mice in anesthetized condition. (A1 and A2) Onset and duration of depression, respectively. (B1 and B2) Similar to A but of persistent gasping. Note that onset of depression in KO mice was significantly delayed by ~15 s from that in WT mice (A1) but the duration of depression in KO mice was shorter by ~80 s than in WT mice (A2), resulting in earlier onset of persistent gasping in KO than in WT mice (B1). (C1 and C2) Similar to A but of terminal gasping. As the duration of persistent gasping of KO mice was much shorter than in WT mice (B2), onset of terminal gasping of KO mice was significantly earlier than in WT mice (C1). Duration of terminal gasping of KO mice was slightly but significantly shorter than that of WT mice (C2). Onset was measured from the time that O_2 concentration actually began to decrease.

with the severity of the hypoxia in wild-type mice. The onset of the terminal gasping declined nearly linearly as the O_2 concentration was lowered within the range of testing (4.5–7.0% O_2) (Fig. 12D, correlation coefficient 0.87).

The KO mice also showed persistent and terminal gasping [insets (2) and (3), respectively, in Fig. 11, B1]. However, the period of stable gasping seldom persisted [compare inset (1) to (3) in Fig. 11, A1 and B1]. In addition, the onset of terminal gasping in KO mice was significantly earlier than in wild-type mice (Fig. 12C) and did not change regardless of the O_2 concentration (Fig. 12D, correlation coefficient 0.21), indicating an inability of the KO mice to regulate the hypoxic response according to the severity of the hypoxia in that range of O_2 concentration (see also Supplementary material, Fig. S1).

As mentioned, there was no difference in onset or duration (peak period) of tachypnea in wild-type and KO mice. In addition, the onset of initial depression was similar in both types of mice. Thus, the dependency of onset of terminal gasping on the severity of hypoxia (Fig. 12D) suggests that maintenance of hypoxic responses from onset of depression to the end of persistent gasping is regulated in an O_2-level-sensitive manner in wild-type but not KO mice. Thus, considering both the anesthetized and unanesthetized experiments, it is clear that Kir6.2-containing K_{ATP} channels are critically involved in the maintenance of depression and gasping during severe hypoxic conditions.

Discussion

Gasping appears clinically when the blood O_2 content is reduced to ~25% of the normal level, and is readily distinguished from eupnea by the large opening of the lower jaw and long interbreath interval. This distinct breathing pattern can persist for minutes or hours, assuring minimum ventilation until the blood oxygenation state is improved, but the molecular basis of the maintenance of gasping is poorly understood. In the present study, each of the hypoxic responses seen in wild-type mice could be generated in Kir6.2 KO mice but the duration of depression and gasping, and not of tachypnea and sigh was significantly shorter in KO than in wild-type mice in the anesthetized condition. In addition, the total duration from onset of depression to terminal gasping in KO mice was unaltered by the O_2 deprivation level within the range of testing (4.5–7.0% O_2) in unanesthetized condition, whereas total duration clearly depended upon the severity of the hypoxia in wild-type mice.

Contribution of central vs. peripheral ATP-sensitive potassium channels in hypoxia-induced respiratory responses

As KO mice lack K_{ATP} channels in the whole body, involvement of the peripheral K_{ATP} channels in the control of severe hypoxia-induced respiratory responses including gasping cannot be excluded. In particular, heart and skeletal muscle K_{ATP} channels, consisting of Kir6.2 and SUR2A subunits (Inagaki *et al.*, 1996), might contribute to the hypoxic responses. However, the difference in gasping between the wild-type and KO isolated head cannot be explained by the cardiac K_{ATP} channels. In addition, mice lacking vascular smooth muscle-type K_{ATP} channels containing Kir6.1 subunits exhibited gasping responses similar to those of wild-type mice when decapitated, suggesting that the Kir6.2-containing K_{ATP} channels in the central nervous system are crucial in the regulatory mechanism of gasping. Indeed, it has been reported that the time to last gasp following decapitation and that following exposure to systemic anoxia are similar in newborn rats when the body temperature is equalized (Fewell, 2005), indicating the

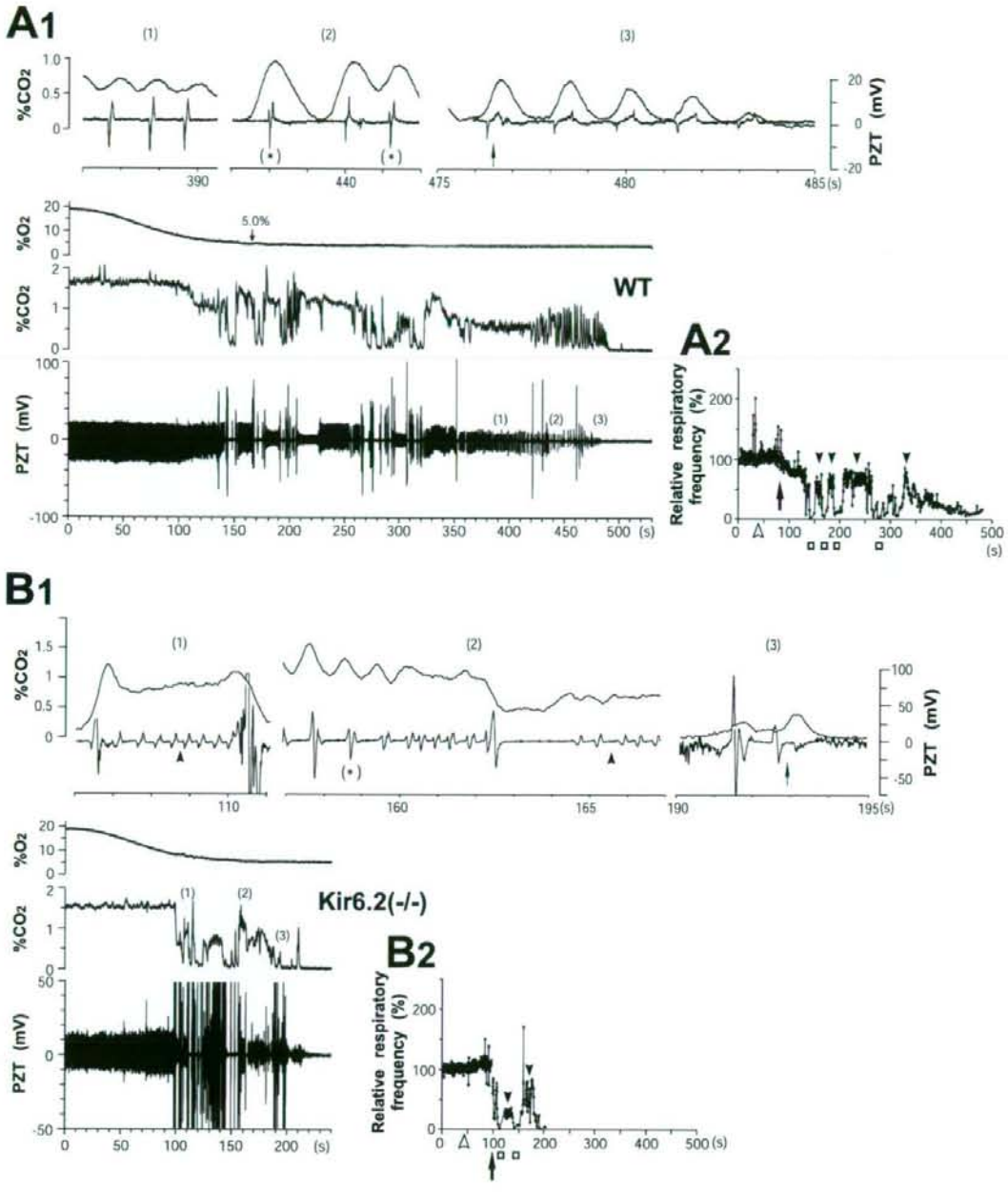

FIG. 11. Typical changes in respiration of mice subjected to severe hypoxia (4.5–5.0% O_2) in unanesthetized condition. Raw traces of respiratory responses (A1) and changes in the respiratory frequency relative to the mean frequency before hypoxic challenge (A2) of wild-type (WT) mouse subjected to 4.8% O_2. Hypoxia was imposed very slowly to compare gasping of WT with that of knockout (KO) mice (see Results). The response, which followed periods of tachypnea (onset, open arrowhead in A2) and the initial depression (onset, filled arrow in A2), consisted of irregularly mixed depression (filled arrowheads in A2) and apnea-like periods (open squares in A2) frequently accompanying large body movement [extraordinarily large deflections in the piezoelectric transducer (PZT) trace in A1]. A stable, slow rhythm then emerged [inset (1)] and persisted until terminal breaths [inset (3), thin arrow]. During this slow rhythm, the PZT shape (lower trace in the insets) showed characteristics of either biphasic [inset (1)] or triphasic [asterisks in parentheses in inset (2)] persistent gasping. During the terminal breaths, a PZT shape characteristic of terminal gasping is seen [inset (3), thin arrow]. The polarity of the PZT deflection is affected by the posture of the mouse. Note that changes in percentage CO_2 correlated well with those of PZT responses. As a change in posture caused fluctuations in the response time of the percentage CO_2, CO_2 traces in the insets (above traces) were arranged to be readily correlated to individual PZT deflections. (B1 and B2) Similar to A but of a KO mouse subjected to 5.0% O_2. The hypoxic responses were irregular and persisted for only a short period. Filled arrowheads in insets (1) and (2) denote depression. Thin arrow in inset (3) denotes a terminal gasp showing an atypical PZT shape. Traces of respiratory frequency were discontinuous at some points due to large spontaneous body movements masking the breath.

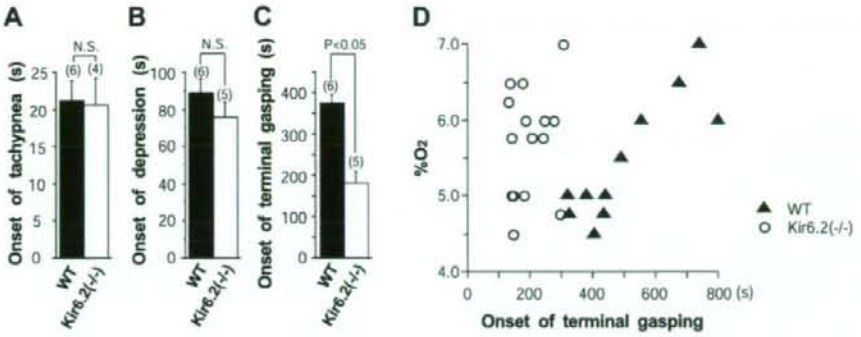

FIG. 12. Quantitative comparison of respiratory responses during hypoxia of wild-type (WT) and knockout (KO) mice in unanesthetized condition. (A–C) Comparison of onset of tachypnea, initial depression and terminal gasping, respectively, for very severe hypoxia (4.5–5.0% O_2). No significant difference was detected in the onset of tachypnea. The onset of the initial depression of KO mice was similar to that of WT mice. In contrast, terminal gasping of WT mice began significantly later than that of KO mice, demonstrating long duration of hypoxic response including depression, apnea and gasping in WT mice. (D) Onset of terminal gasping plotted against percentage O_2 (4.5–7.0%). The gasping onset of WT mice shortened linearly as the O_2 concentration was lowered, whereas those in KO mice were unaltered regardless of the concentrations within the range. Onset was measured from the time that the O_2 concentration began to decrease. N.S., not significant.

critical importance of central regulation in the maintenance of severe hypoxia-induced gasping.

Regarding the control of hypoxic gasping, the K_{ATP} channels in peripheral chemoreceptors such as the carotid body could also be involved. However, this is unlikely as the pattern of gasping and the magnitude of phrenic bursts during gasping are not altered by carotid sinus nerve stimulation (Neubauer *et al.*, 1990). In addition, initiation of gasping is not affected by sympathetic or parasympathetic blockade, such as intracarotid administration of NaCN, indicating a central regulation mechanism independent of autonomic integrity (St. John & Knuth, 1981; Sanocka *et al.*, 1992). Indeed, Kir6.2 mRNA was not detected in the carotid body of mice, although Kir6.1 mRNA was abundantly detected (data not shown).

Influence of CO_2 on gasping

Although gasping in the present study could result from hypocapnia rather than hypoxia, this is unlikely as neither the frequency nor the intensity of gasps was reported to be altered by hypocapnia (St. John & Knuth, 1981). In addition, it is known that phrenic nerve activity during gasping is not altered by reducing the end-tidal partial pressure of CO_2 from normocapnic to various hypocapnic levels (St. John & Knuth, 1981). Other investigators have also reported that the pattern of gasping and the magnitude of phrenic bursts during gasping are not altered by hypercapnea (Neubauer *et al.*, 1990). Indeed, in our experiment, the difference in gasping between KO and wild-type mice under isocapnic hypoxia by 92% N_2/3% CO_2/5% O_2 was similar to that detected by 95% N_2/5% O_2 (data not shown).

Hypoxia-induced sighs and apnea-like period

In the initial hypoxic period under anesthetized condition, both wild-type and KO mice showed similar onset and numbers of sighs, indicating that Kir6.2-containing K_{ATP} channels are not required for the initiation or maintenance of sighs, although their involvement in the modification of rhythmicity or relative amplitude cannot be excluded.

Regarding the apnea-like period between sighs following tachypnea in KO mice, no such period was detected in wild-type mice under anesthetized condition. In addition, it is noted that very fast breathing-like motions could be detected by PZT during a portion of the apnea-like period.

In unanesthetized condition, apnea (Fig. 11, A2) was detected not only in KO but also in wild-type mice in the middle stage of hypoxia. It is thus of interest to determine if the very fast breathing-like motions occur during apnea in the conscious state, and whether this is related to the similar peak period of tachypnea and onset of depression observed in both types of mice in unanesthetized condition.

Definition of gasping in mice

Among the conventionally used criteria of gasping, the rapid rise-time of integrated phrenic bursts is reported to be inappropriate in small mammals such as mice for distinguishing gasping from eupnea (Fukuda, 2000; St. John & Paton, 2003). In the present study, we included data on expiratory activity detected by PZT and divided gasping in the anesthetized condition in adult mice into persistent gasping of biphasic PZT shape and terminal gasping of wide phrenic bursts. Discrimination of the period of persistent gasping from that of depression was based on the symmetry and stability of the PZT shape, which reflects the balance between inspiratory and expiratory body movement detected by the vertical motion of the PZT.

In addition, gasping shown by triphasic shape was detected in the unanesthetized condition. Distinct types of gasping have also been reported by Gozal *et al.* (1996) with whole body plethysmography of immature rats in an alert condition. Prolonged, severe hypoxia elicited a triphasic ventilation consisting of an initial expiration followed by an inspiration and a second expiration (type I gasps), and a biphasic ventilation consisting of a prominent initial inspiration followed by a small expiration (type II gasps) (Gozal *et al.*, 1996). In their study, no biphasic gasping of symmetrical shape corresponding to persistent gasping was mentioned. The relationship between triphasic and biphasic gasping, and how expiration contributes to gasping are also of interest.

Mechanism of gasping

The cellular mechanisms underlying eupnea and gasping have been discussed extensively (Ramirez *et al.*, 1998; Koshiya & Smith, 1999; Lieske *et al.*, 2000; Del Negro *et al.*, 2002; Ramirez & Lieske, 2003; St. John & Paton, 2003; Pena *et al.*, 2004; Paton *et al.*, 2006). It is

proposed that gasping depends on intrinsic cellular mechanisms localized in the pre-Botzinger complex in the medulla, especially persistent sodium channel-dependent cellular properties (Del Negro *et al.*, 2002; Pena *et al.*, 2004; Paton *et al.*, 2006), whereas eupnea depends on the complex interaction of neuronal networks in the brainstem, either restricted or not restricted to the pre-Botzinger complex. Selective lesioning of the pre-Botzinger complex eliminates eupneic breathing but not gasping (Ramirez *et al.*, 1998), suggesting a complex nature of gasping *in vivo*. It has been reported that K_{ATP} channels comprising Kir6.2/SUR1 but not Kir6.1/SUR2 are expressed in inspiratory neurons in the pre-Botzinger complex by single-cell antisense RNA amplification-polymerase chain reaction (Haller *et al.*, 2001). Thus, it is of interest to clarify the participation of K_{ATP} channels in the regulation of hypoxic ventilatory responses.

The present results using KO mice lacking Kir6.2 indicate that these K_{ATP} channels are not essential for generating eupnea, sighs and gasping but rather are critically involved in maintaining a level of gasping and depression proportionate to the severity of the hypoxia, which might well be essential in recovery by reoxygenation (Neubauer *et al.*, 1990). In addition, of the hypoxia-induced ventilatory responses, only gasping and depression but not sigh were critically affected in KO mice, suggesting an alternative mechanism of control of sighs. The combination of recordings of phrenic nerve activity and PZT responses in spontaneously breathing animals highlights the importance of expiratory as well as inspiratory patterns in classifying depression and gasping.

It is proposed that the duration of survival of neurons in the respiratory centres after decapitation is determined by the balance between the anoxic energy reserve and the cerebral metabolic rate (Thurston *et al.*, 1978). Opening of the K_{ATP} channels, which couple the intracellular metabolic state with electrical activity, could well minimize energy consumption to protect the brain in such conditions (Ballanyi, 2004; Yamada & Inagaki, 2005). Further investigation is required to clarify how K_{ATP} channels participate in the central regulation of depression and gasping under severe hypoxia.

Supplementary material

The following supplementary material may be found on www.blackwell-synergy.com

Fig. S1. Typical changes in respiration of wild-type and knockout mice subjected to hypoxia without anesthesia.

Acknowledgements

This work was supported by Grant-in-aid for Scientific Research (15590181), JSPS Fellows (1650112), and Creative Scientific Research (15GS0301) from the Ministry of Education, Culture, Sports, Science and Technology of Japan. We are grateful to Drs Shinichi Sato, Masanori Nakata, Ya-Juan Zheng, Katsuaki Yoshizaki, Ms Kana Kato and Ms Emiko Harada (Akita University) for technical help.

Abbreviations

K_{ATP} channel, ATP-sensitive potassium channel; KO, knockout; PZT, piezoelectric transducer; SUR, sulfonylurea receptor.

References

Ashcroft, F.M. (1988) Adenosine 5′-triphosphate-sensitive potassium channels. *Annu. Rev. Neurosci.*, **11**, 97–118.

Ballanyi, K. (2004) Protective role of neuronal K_{ATP} channels in brain hypoxia. *J. Exp. Biol.*, **207**, 3201–3212.

Del Negro, C.A., Morgado-Valle, C. & Feldman, J.L. (2002) Respiratory rhythm: an emergent network property? *Neuron*, **34**, 821–830.

Fazekas, J.F., Alexander, F.A.D. & Himwich, H.E. (1941) Tolerance of the newborn to anoxia. *Am. J. Physiol.*, **134**, 281–287.

Fewell, J.E. (2005) Protective responses of the newborn to hypoxia. *Resp. Physiol. Neurobiol.*, **149**, 243–255.

Fukuda, Y. (2000) Respiratory neural activity responses to chemical stimuli in newborn rats: reversible transition from normal to 'secondary' rhythm during asphyxia and its implication for 'respiratory like' activity of isolated medullary preparation. *Neurosci. Res.*, **38**, 407–417.

Gang, S., Sato, Y., Kohama, I. & Aoki, M. (1995) Afferent projections to the Botzinger complex from the upper cervical cord and other respiratory related structures in the brainstem in cats: retrograde WGA-HRP tracing. *J. Auton. Nerv. Syst.*, **56**, 1–7.

Gozal, D., Torres, J.E., Gozal, Y.M. & Nuckton, T.J. (1996) Characterization and developmental aspects of anoxia-induced gasping in the rat. *Biol. Neonate*, **70**, 280–288.

Haller, M., Mironov, S.L., Karschin, A. & Richter, D.W. (2001) Dynamic activation of K_{ATP} channels in rhythmically active neurons. *J. Physiol. (Lond.)*, **537**, 69–81.

Holowach-Thurston, J., Hauhart, R.E. & Jones, E.M. (1974) Anoxia in mice: reduced glucose in brain with normal or elevated glucose in plasma and increased survival after glucose treatment. *Pediat. Res.*, **8**, 238–243.

Inagaki, N., Gonoi, T., Clement, J.P., Namba, N., Inazawa, J., Gonzalez, G., Aguilar-Bryan, L., Seino, S. & Bryan, J. (1995) Reconstitution of IKATP: An inward rectifier subunit plus the sulfonylurea receptor. *Science*, **270**, 1166–1170.

Inagaki, N., Gonoi, T., Clement, J.P., Wang, C.Z., Aguilar-Bryan, L., Bryan, J. & Seino, S. (1996) A family of sulfonylurea receptors determines the pharmacological properties of ATP-sensitive K^+ channels. *Neuron*, **16**, 1011–1017.

Khurana, A. & Thach, B.T. (1996) Effects of upper airway stimulation on swallowing, gasping, and autoresuscitation in hypoxic mice. *J. Appl. Physiol.*, **80**, 472–477.

Koshiya, N. & Smith, J.C. (1999) Neuronal pacemaker for breathing visualized in vitro. *Nature*, **400**, 360–363.

Lieske, S.P., Thoby-Brisson, M., Telgkamp, P. & Ramirez, J.M. (2000) Reconfiguration of the neural network controlling multiple breathing patterns: eupnea, sighs and gasps. *Nat. Neurosci.*, **3**, 600–607.

Miki, T., Nagashima, K., Tashiro, F., Kotake, K., Yoshitomi, H., Tamamoto, A., Gonoi, T., Iwanaga, T., Miyazaki, J. & Seino, S. (1998) Defective insulin secretion and enhanced insulin action in K_{ATP} channel-deficient mice. *Proc. Natl Acad. Sci. U.S.A.*, **95**, 10 402–10 406.

Miki, T., Suzuki, M., Shibasaki, T., Uemura, H., Sato, T., Yamaguchi, K., Koseki, H., Iwanaga, T., Nakaya, H. & Seino, S. (2002) Mouse model of prinzmetal angina by disruption of the inward rectifier Kir6.1. *Nat. Med.*, **8**, 466–472.

Miller, J.A. (1949) Factors of neonatal resistance to anoxia. I. Temperature and survival of guinea pigs under anoxia. *Science*, **110**, 113–114.

Mironov, S.L., Langohr, K., Haller, M. & Richter, D.W. (1998) Hypoxia activates ATP-dependent potassium channels in inspiratory neurones of neonatal mice. *J. Physiol. (Lond.)*, **509**, 755–766.

Mourre, C., Ben Ari, Y., Bernardi, H., Fosset, M. & Lazdunski, M. (1989) Antidiabetic sulfonylureas: localization of binding sites in the brain and effects on the hyperpolarization induced by anoxia in hippocampal slices. *Brain Res.*, **486**, 159–164.

Nakamura, A., Fukuda, Y. & Kuwaki, T. (2003) Sleep apnea and effect of chemostimulation on breathing instability in mice. *J. Appl. Physiol.*, **94**, 525–532.

Neubauer, J.A., Melton, J.E. & Edelman, N.H. (1990) Modulation of respiration during brain hypoxia. *J. Appl. Physiol.*, **68**, 441–451.

Noma, A. (1983) ATP-regulated K+ channels in cardiac muscle. *Nature*, **305**, 147–148.

Paton, J.F.R., Abdala, A.P.L., Koizumi, H., Smith, J.C. & St. John, W.M. (2006) Respiratory rhythm generation during gasping depends on persistent sodium current. *Nat. Neurosci.*, **9**, 311–313.

Pena, F., Parkis, M.A., Tryba, A.K. & Ramirez, J.M. (2004) Differential contribution of Pacemaker properties to the generation of respiratory rhythms during normoxia and hypoxia. *Neuron*, **43**, 105–117.

Ramirez, J.M. & Lieske, S.P. (2003) Commentary on the definition of eupnea and gasping. *Resp. Physiol. Neurobiol.*, **139**, 113–119.

Ramirez, J.M., Schwarzacher, S.W., Pierrefiche, O., Olivera, B.M. & Richter, D.W. (1998) Selective lesioning of the cat pre-Botzinger complex in vivo eliminates breathing but not gasping. *J. Physiol. (Lond.)*, **507**, 895–907.

Sanocka, U.M., Donnelly, D.F. & Haddad, G.G. (1992) Autoresuscitation: a survival mechanism in piglets. *J. Appl. Physiol.*, **73**, 749–753.

Sato, S., Yamada, K. & Inagaki, N. (2006) System for simultaneously monitoring heart and breathing rate in mice using a piezoelectric transducer. *Med. Biol. Eng. Comput.*, **44**, 353–362.

Secher, O. & Wilhjelm, B. (1968) The protective action of anesthetics against hypoxia. *Can. Anaes. Soc. J.*, **15**, 423–440.

Seino, S. (1999) ATP-sensitive potassium channels: a model of heteromultimeric potassium channel/receptor assemblies. *Annu. Rev. Physiol.*, **61**, 337–362.

Selle, W.A. (1944) Influence of glucose on the gasping pattern of young animals subjected to acute anoxia. *Am. J. Physiol.*, **141**, 297–302.

Selle, W.A. & Witten, T.A. (1941) Survival of the respiratory (gasping) mechanism in young animals subjected to anoxia. *Proc. Soc. Exp. Biol. Med.*, **47**, 495–497.

St. John, W.M. & Knuth, K.V. (1981) A characterization of the respiratory pattern of gasping. *J. Appl. Physiol.*, **50**, 984–993.

St. John, W.M. & Paton, J.F.R. (2003) Defining eupnea. *Respir. Physiol. Neurobiol.*, **139**, 97–103.

Thurston, J.H., Hauhard, R.E. & Dirgo, J.A. (1978) Aminophylline increases cerebral metabolic rate and decreases anoxic survival in young mice. *Science*, **201**, 649–651.

Wang, W., Fung, M.L., Darnall, R.A. & St. John, W.M. (1996) Characterizations and comparisons of eupnoea and gasping in neonatal rats. *J. Physiol. (Lond.)*, **490**, 277–292.

Yamada, K. & Inagaki, N. (2005) Neuroprotection by K_{ATP} channels. *J. Mol. Cell. Cardiol.*, **38**, 945–949.

Yamada, K., Ji, J.J., Yuan, H., Miki, T., Sato, S., Horimoto, N., Shimizu, T., Seino, S. & Inagaki, N. (2001) Protective role of ATP-sensitive potassium channels in hypoxia-induced generalized seizure. *Science*, **292**, 1543–1546.

Available online at www.sciencedirect.com
ScienceDirect
Biochemical and Biophysical Research Communications 353 (2007) 40–46
BBRC
www.elsevier.com/locate/ybbrc

Adult pancreatic islets require differential pax6 gene dosage

Akihiro Hamasaki [a], Yuichiro Yamada [a,b,*], Takeshi Kurose [a], Nobuhiro Ban [c], Kazuaki Nagashima [a], Akira Takahashi [a], Shimpei Fujimoto [a], Dai Shimono [a], Michio Fujiwara [d], Shinya Toyokuni [e], Yutaka Seino [a,f], Nobuya Inagaki [a,g]

[a] *Department of Diabetes and Clinical Nutrition, Kyoto University Graduate School of Medicine, Kyoto, Japan*
[b] *Department of Internal Medicine, Division of Endocrinology, Diabetes and Geriatric Medicine, Akita University School of Medicine, Akita, Japan*
[c] *Department of Physiology, Akita University School of Medicine, Akita, Japan*
[d] *Drug Safety Research Laboratories, Astellas Pharma Inc., Osaka, Japan*
[e] *Department of Pathology and Biology of Disease, Kyoto University Graduate School of Medicine, Kyoto, Japan*
[f] *Kansai Electric Power Hospital, Osaka, Japan*
[g] *CREST of Japan Science and Technology Cooperation (JST), Kyoto, Japan*

Received 15 November 2006
Available online 4 December 2006

Abstract

Pax6, a paired homeodomain transcription factor, plays crucial roles in morphogenesis of eye, central nervous system, and pancreatic islets. Recently, heterozygosity for pax6 mutation has been reported in some individuals with glucose intolerance and aniridia. To investigate the role of pax6 for pancreatic islet function, we examined the pancreatic phenotype of small eye rat strain (rSey^2) with a point mutation in the pax6 locus resulting in truncated PAX6 proteins. Analyses of the insulin secretory profile of heterozygous rSey^2/+ revealed that insulin secretion is significantly increased in response to membrane-depolarizing stimuli such as arginine, tolbutamide, and KCl. The processes of insulin granule exocytosis were suggested to be enhanced in rSey^2/+. On the other hand, pancreatic insulin and glucagon content and islet architecture in rSey^2/+ showed no significant differences compared to wild-type. These findings indicate differential requirements for pax6 gene dosage in displaying function and maintaining architecture of adult pancreatic islets.

Keywords: Pax6; Pancreatic islets; Insulin secretion; Arginine; Small eye; Pancreas

Transcription factors playing a role in pancreatic development have been shown to orchestrate the process of cell differentiation and transition by regulating the expression of numbers of genes [1,2]. To form the pancreas and organize pancreatic islets, multiple transcription factors play roles at precise steps in the developmental program. Various models in which these transcription factors are inactivated have revealed defects of pancreatic development or pancreatic islet morphogenesis.

The paired homeobox (Pax) family of transcription factors is involved in embryonic development of many organs including eyes, brain, kidney, thyroid gland, immune system, and the pancreas [3,4]. Two of its members, Pax4 and Pax6, play important roles in pancreatic endocrine cell differentiation [5,6]. In addition, Pax6 is essential for the development of eye and central nervous system and regulates the expression of various functional molecules in these tissues [7]. During the mouse embryogenesis, PAX6 protein can be detected already around E9.0 in the pancreatic endoderm, and its expression is maintained throughout pancreas development in all endocrine cells [8]. Analyses of pax6 mutant animals (Fig. 1) have revealed that differentiation of endocrine cells and the forming of proper islet architecture are severely affected in the fetal pancreas in the homozygous state. Pax6 knockout mice lack glucagon-producing α-cells and do not form proper islet structure [6]. In Sey^{NEU} mice, in which the PAX6 protein is

* Corresponding author.
E-mail address: yamada@gipc.akita-u.ac.jp (Y. Yamada).

0006-291X/$ - see front matter © 2006 Elsevier Inc. All rights reserved.
doi:10.1016/j.bbrc.2006.11.105

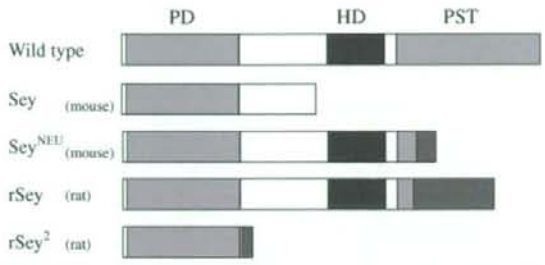

Fig. 1. Schematic diagram of coding region of pax6 gene and mutants. Wild-type PAX6 has a paired domain (PD), homeodomain (HD), and proline/serine/threonine rich transactivation domain (PST). Sey^{NEU} and rSey have a mutation, which results in a PAX6 protein that has a PD and HD but lacks the functional PST domain. Sey and rSey^{2} (this study) have a mutation resulting in a PAX6 that has a PD but lacks the HD and PST domain completely.

truncated directly after the homeodomain, all four endocrine cell types are decreased in number [9]. Thus, Pax6 is involved in pancreatic development, particularly in endocrine cell differentiation and pancreatic islet organogenesis.

Transcription factors are involved not only in regulating pancreas development but also in pancreatic endocrine cell function. Many mutation models of transcription factors have shown that these mutations influence β-cell molecular events and the insulin secretory profile by altering the gene expression.

However, the role of PAX6 in adult islet function is little known except for the observations *in vitro* that PAX6 increases insulin, somatostatin, and glucagon gene transcription by binding with their promoters [9,10], and is involved in the regulation of enzymes and transcription factors [11,12]. The homozygous mice of pax6 knockout, Sey^{NEU} lack eyes and even model mice with conditional inactivation of pax6 in the endocrine pancreas [13] die shortly after birth, limiting the analyses of PAX6 function in the postnatal pancreatic islet function.

To investigate the mechanisms by which alterations in PAX6 affect islet function, we examined pancreatic islet function and architecture in small eye rat strain (rSey^{2}) with point mutation in the pax6 locus resulting in truncated PAX6 proteins [14] and found that in contrast to showing normal insulin secretion in response to glucose, rSey^{2}/+ showed surprisingly increased insulin release in response to membrane depolarizing stimuli and that rSey^{2}/+ had normal pancreatic islet architecture, indicating different requirement for pax6 gene dosage in the function and the morphology of the pancreatic islets.

Materials and methods

Animals. Mutant rats with small eyes (rSey^{2}) [14] were used in this study. Studies for the adult rats were performed in heterozygous (rSey^{2}/+) and their age-matched wild-type littermates. Homozygous rat embryos were obtained by inter-crossing male and female heterozygotes. Animal care and procedures were approved by the Animal Care Committee of Kyoto University.

Measurement of blood glucose, insulin, and glucagon levels. Blood glucose levels were measured by enzyme-electrode method. Plasma insulin levels were measured using ELISA kit (Shibayagi, Gunma, Japan). Plasma glucagon levels were measured using ELISA kit (Yanaihara Institute Inc., Shizuoka, Japan). Different groups of age-matched 20- to 24-week-old male rats were used for intraperitoneal glucose tolerance test. After an overnight fast, plasma insulin, glucagon, and glucose levels were measured and D-glucose (2 g/kg body weight) was loaded. In the insulin tolerance test, human insulin (1 U/kg) was injected subcutaneously in the fed condition. Blood samples were taken from the tail vein at indicated times.

Quantification of pancreatic peptide content. Protein was extracted from the dissected pancreas using acid extraction. Protein content was measured by Bio-Rad protein assay (Bio-Rad Laboratories, Hercules, CA). The amount of immunoreactive insulin was determined by RIA, using rat insulin as described [15]. The amount of immunoreactive glucagon was determined by using RIA kit (Linco Research, St. Charles, MO).

Immunohistochemistry. The pancreata of rats were removed under pentobarbital anesthesia (40 mg/kg body weight) and fixed in Bouin's solution. Pancreatic specimens were embedded in paraffin and sectioned at 3.5 μm. The avidin–biotin complex method with alkaline phosphatase or with peroxidase was used as previously described [16] with a slight modification. After deparaffinization, the following were sequentially applied: normal goat or rabbit serum (diluted to 1:75, Dako, Kyoto, Japan), primary antibodies, biotin-labeled goat anti-rabbit or rabbit anti-goat IgG serum (diluted to 1:300, Dako), and avidin–biotin–alkaline phosphatase complex or avidin–biotin–peroxidase complex (diluted to 1:100, Vector Laboratories, Burlingame, CA), followed by hematoxylin nuclear counterstaining. Staining was visualized in black and red by alkaline phosphatase substrate (Vector Laboratories) and in brown by peroxidase substrate. For PAX6 analysis, paraffin sections of pancreata were deparaffinized and autoclaved for 10 min at 121 °C in 10 mM citrate buffer (pH 6.0). The following primary antibodies were used: rabbit anti-insulin polyclonal antibody (diluted to 1:350, Dako), rabbit anti-glucagon serum (diluted to 1:500, OAL-123, Otsuka Assay Laboratory, Tokushima, Japan), rabbit anti-somatostatin polyclonal antibody (diluted to 1:200, Dako), rabbit anti-pancreatic polypeptide polyclonal antibody (diluted to 1:200, Dako), goat anti-GLUT2 polyclonal antibody (diluted to 1:50, C-19, Santa Cruz Biotechnology, Santa Cruz, CA) or rabbit anti-PAX6 polyclonal antibody (diluted to 1:20, H-295, Santa Cruz Biotechnology).

Isolated pancreatic perfusion. The pancreas was isolated as previously described [17]. All perfusions were accomplished with Krebs–Ringer Bicarbonate Buffer (KRBB) containing 0.25% bovine serum albumin (BSA, Fraction V, Sigma, St. Louis, MO) and 4.6% dextran (mean molecular weight 70,000; Pharmacia, Uppsala, Sweden). The perfusate was gassed with 95% O_2–5% CO_2 to maintain pH 7.4 at 37 °C. The flow rate was kept constant at 1.9 ml/min. After 20 min of equilibration, the perfusate was collected at 1-min intervals by cannula inserted into the portal vein. The collected effluent was frozen immediately with 1000 U aprotinin (Bayer, Leverkusen, German). The amount of immunoreactive insulin and immunoreactive glucagon was determined by RIA as described above.

Measurement of insulin release from isolated rat pancreatic islets. Isolated islets were cultured for 18 h in RPMI 1640 medium containing 10% fetal calf serum (FCS), 100 U/ml penicillin, and 100 μg/ml streptomycin. Insulin release from intact islets was monitored using batch incubation system described previously [18] with slight modifications. Cultured islets were preincubated at 37 °C for 30 min in KRBB supplemented with 2.8 mM glucose, 0.2% BSA, and 10 mM Hepes, adjusted to pH 7.4. Groups of 10 islets were then batch-incubated for 30 min in 0.4 ml of KRBB with test materials. The amount of immunoreactive insulin was determined by RIA as described above.

Measurement of intracellular Ca^{2+}. For intracellular Ca^{2+} ($[Ca^{2+}]_i$) measurement, cultured islets were loaded with fura-PE3 during 2 h of preincubation in the presence of 2 μM fura-PE3AM (Calbiochem, La Jolla, LA) as previously described [18]. Islets were placed at 36 ± 1 °C, superfused with KRBB containing 2.8 mM glucose and 10 mM Hepes adjusted to pH 7.4 for 30 min, and subsequently exposed to the medium containing a high concentration of K^+. The islets were excited successively